

1 **Genomic architecture of phenotypic plasticity of complex traits in tetraploid wheat in**
2 **response to water stress**

3 Andrii Fatiukha^{1,2}, Mathieu Deblicq³, Valentina Klymiuk^{1,2}, Lianne Merchuk-Ovnat⁴, Zvi
4 Peleg⁴, Frank Ordon³, Tzion Fahima^{1,2}, Abraham B. Korol^{1,2}, Yehoshua Saranga⁴, Tamar
5 Krugman¹.

6 ¹Institute of Evolution, University of Haifa, Haifa, Israel; ²Department of Evolutionary and
7 Environmental Biology, University of Haifa, Haifa, Israel; ³Julius Kühn-Institut (JKI) Federal
8 Research Centre for Cultivated Plants, Institute for Resistance Research and Stress Tolerance,
9 Quedlinburg, Germany; ⁴R. H. Smith Institute of Plant Science & Genetics in Agriculture, The
10 Hebrew University of Jerusalem, Rehovot, Israel.

11 Running title: Genomic architecture of phenotypic plasticity in wheat in response to water stress

12

13 Author for correspondence:

14 *Tamar Krugman*

15 *Tel: 972-04-8240783*

16 *Email: tkrugman@evo.haifa.ac.il*

17

18 The date of submission: 02.03.2019

19 The number of tables: 3

20 The number of figures: 4 (Figures 2 and 4 should be in colour in print, Figures 1 and 3 should be
21 in colour online-only)

22 The number of supplementary tables: 17

23 The number of supplementary figures: 19

24 The word count: 6493

25

26 **Highlight**

27 The study presents a new approach for quantification of plant adaptation to various stresses and
28 provides new insights into the genetic basis of wheat complex traits under water-deficit stress.

29 **Abstract**

30 Phenotypic plasticity is one of the main mechanisms of adaptation to abiotic stresses via changes
31 in critical developmental stages. Altering flowering phenology is a key evolutionary strategy of
32 plant adaptation to abiotic stresses in order to achieve maximum possible reproduction. The
33 current study is the first to apply the linear regression residuals as a drought plasticity scores,
34 while taking into account the differences in flowering phenology and trait variation under non-
35 stress conditions. We characterized the genomic architecture of 17 complex traits and their
36 drought plasticity using a mapping population derived from a cross between durum wheat
37 (*Triticum durum*) and wild emmer wheat (*T. dicoccoides*). We identified 79 QTLs, of which 33
38 were plastic in response to water stress and exhibited epistatic interactions and/or pleiotropy
39 between the initial and plasticity traits. *Vrn-B3* (*TaTF1*) residing within an interval of a major
40 drought-escape QTL was proposed as a candidate gene. The favorable alleles for most of the
41 plasticity QTLs were contributed by wild emmer, demonstrating the high potential of wild
42 relatives for wheat improvement. Our study presents a new approach for quantification of plant
43 adaptation to various stresses and provides new insights into the genetic basis of wheat complex
44 traits under water-deficit stress.

45 **Key words:** drought resistance strategies, flowering phenology, genomic architecture, linear
46 regression, phenotypic plasticity, QTL analysis, wild emmer wheat.

47 **Introduction**

48 Water stress is one of the main abiotic factors affecting plant growth and limiting crop
49 production. Global climate changes increase the frequency of extreme drought events in many
50 regions, thus becoming a severe threat to food security (Leng *et al.*, 2015; Mann andand Gleick,
51 2015; Nam *et al.*, 2015). Wheat is one of the most important crops worldwide, providing about
52 20% of calories and proteins in human consumption (FAOSTAT). Drought affects more than
53 42% of the worldwide wheat production area (Kosina *et al.*, 2007); hence, the improvement of
54 drought resistance in wheat cultivars is among the main targets for wheat breeders.

55 Crop wild relatives developed adaptation mechanisms to cope with water-limited conditions that
56 can be used for crop improvement (Henry andand Nevo, 2014). Wild emmer wheat (WEW)
57 (*Triticum dicoccoides*) germplasm represents an important reservoir of genetic variation for
58 useful traits. It can increase the genetic diversity available to breeders for wheat improvement,
59 including resistance to abiotic and biotic stresses (Levy and Feldman, 1987; Nevo *et al.*, 2002;
60 Peleg *et al.*, 2005, 2009; Huang *et al.*, 2016). Previously, we have evaluated WEW populations,
61 representing an aridity gradient across Israel and vicinity, and revealed high diversity for drought
62 stress tolerance with some genotypes displaying better performance under drought than durum
63 wheat cultivars (Peleg *et al.*, 2005). Then, we developed a mapping population derived from a
64 cross between durum and WEW and genetically dissected drought-adaptive loci (Peleg *et al.*,
65 2009). Subsequently, several WEW chromosomal regions conferring increased yield and
66 drought-adaptive traits were introgressed into wheat cultivars using marker assisted selection
67 approach (Merchuk-Ovnat *et al.*, 2016a, 2016b, 2017). We also conducted whole transcriptome
68 analyses of drought tolerant *versus* drought susceptible accessions of WEW in response to water
69 stress (Krugman *et al.*, 2010, 2011).

70 The complex responses of plants to water stress encompass multiple physiological, cellular and
71 biochemical processes, coordinated by a large number of genes (Mickelbart *et al.*, 2015). Due to
72 the complex quantitative mode of inheritance of traits involved in response to drought stress and
73 their effect on productivity traits, unraveling the genomic architecture of these traits is crucial for
74 further progress in this field. Currently, the most suitable approach for genetic dissection of
75 complex traits, such as drought resistance, is quantitative trait loci (QTL) analysis (Tardieu and
76 Tuberosa, 2010; Blum, 2011; Lopes *et al.*, 2014b; Mickelbart *et al.*, 2015). QTL analysis of

77 physiological drought adaptive traits (DAT) associated with response to drought can be used for
78 genetic dissection of drought resistance strategies such as escape, avoidance or tolerance, as
79 demonstrated in recent publications (Rebetzke *et al.*, 2008; Adiredjo *et al.*, 2014; Borrell *et al.*,
80 2014; Blum, 2017). However, only a few studies were focused on the effect of physiological
81 traits on productivity, taking into account the interaction between yield related traits and DAT
82 (Pinto *et al.*, 2010; Ahmad *et al.*, 2014; Graziani *et al.*, 2014; Mwadzingeni *et al.*, 2016b).

83 Phenotypic plasticity is one of the ways of plants to respond to environmental stress; therefore, a
84 better understanding of this phenomenon can help to improve crop management (Nicotra *et al.*,
85 2010; Bloomfield *et al.*, 2014). Several approaches for QTL analyses can be used for the
86 identification of genomic regions that confer phenotypic plasticity in response to abiotic stress:
87 (a) testing of QTL-by-environment interactions (Messmer *et al.*, 2009); (b) mapping of QTLs for
88 plasticity response (Lacaze *et al.*, 2009; Adiredjo *et al.*, 2014); (c) using a multi-environmental
89 approach (MEA) in QTL analysis (van Eeuwijk *et al.*, 2010); or (d) QTL mapping of a
90 susceptibility index calculated for each trait (Peleg *et al.*, 2009). Changes in flowering phenology
91 play an important and decisive role in plant development and plasticity in response to water
92 stress (Kamran *et al.*, 2014; Riboni *et al.*, 2014; Kazan and Lyons, 2016). Therefore, to reduce
93 various biases in QTL analysis, the influence of flowering time should be taken into account
94 when analyzing other traits. The simplest way to solve this problem is to use mapping
95 populations with a narrow distribution of flowering time. Alternatively, the mapping population
96 can be divided into smaller subsets of individuals by their range of flowering (Pinto *et al.*, 2010).
97 Another approach is to include various quantitative adjustments of variation in flowering time
98 for QTL mapping of other traits (Sabadin *et al.*, 2012; Hill *et al.*, 2013; Lopes *et al.*, 2014a;
99 Onogi *et al.*, 2016). Previously, deviations from the regression line (i.e., residuals) were defined
100 as drought resistant indexes (DRI) for a set of pearl millet cultivars, independently of the effect
101 of heading time and yield potential under control conditions (Bidinger *et al.*, 1982). However,
102 despite its simplicity, this approach has not been utilized in QTL mapping.

103 In the current study, we applied QTL mapping of phenotypic plasticity of complex traits under
104 water-limited conditions using a recombinant inbred line (RIL) population derived from a cross
105 between durum wheat (*Triticum durum*) and drought resistant WEW. For QTL analysis, we
106 targeted groups of traits related to: (a) yield; (b) phenology; (c) morphology; (d) biomass; and (e)

107 drought-adaptive physiological traits (DAT). We employed residuals of linear regression
108 between values of traits in control and stress conditions as drought plasticity traits. Wide
109 distribution of heading time in the population was taken into account to reduce various biases in
110 QTL analysis of the traits. We further used the whole genome assembly of WEW (Avni *et al.*,
111 2017) for localization of candidate genes (CGs) associated with the studied traits, residing within
112 the QTL intervals, including regulation of flowering and development.

113 **Materials and Methods**

114 **Plant material and growth conditions**

115 The RIL population (150 F₆ lines) was derived from a cross between durum wheat (*T. durum*, cv.
116 Langdon; LDN hereafter) and WEW (accession G18-16), developed by single-seed descent;
117 hereafter referred to as G×L population (described by Peleg *et al.* 2009). The continuous water-
118 deficient experiment was conducted in an insect-proof screen-house protected by a polyethylene
119 top, at the experimental farm of the Hebrew University of Jerusalem in Rehovot, Israel (34°47'N,
120 31°54'E; 54 m above sea level). Two irrigation regimes were applied: well-watered (WW, 750
121 mm control) and water-limited (WL, 350 mm), irrigated with drip water system. A split-plot
122 factorial (RIL × irrigation regime) block design with three replicates was employed; each block
123 consisted of two main plots (for the two irrigation regimes), with main plots split into subplots as
124 described in Peleg *et al.* (2009).

125 **DNA extraction and SNP genotyping**

126 DNA was extracted from fresh leaf tissue of the parental genotypes (LDN and G18-16) and from
127 a pooled sample of each of the 150 F₆ RILs following a standard CTAB protocol (Doyle, 1991).
128 DNA was normalized to 50 ng/μl. Single nucleotide polymorphism (SNP) genotyping was
129 performed using the Illumina Infinium 15K Wheat platform, developed by TraitGenetics,
130 Gatersleben, Germany (Muqaddasi *et al.*, 2017), consisting of 12,905 SNPs selected from the
131 wheat 90K array (Wang *et al.*, 2014).

132 **Phenotypic traits**

133 Four sets of phenotypic traits were used in present the QTL analysis: one set of *initial traits* and
134 three sets of *derivative traits*. The *initial* set included 17 traits of which 13 were previously

135 measured in the population under water-limited and well-watered conditions (described by Peleg
136 *et al.* 2009, 2011): grain yield (GY); thousand kernel weight (TKW); kernel number per spike
137 (KNSP); harvest index (HI); spike dry matter (SpDM); total dry matter (TotDM); carbon isotope
138 ratio ($\delta^{13}\text{C}$); osmotic potential (OP); chlorophyll content (Chl); flag leaf rolling (LR); culm
139 length (CL); days from planting to heading (DP-H); days from heading to maturity (DH-M).
140 Four additional traits included: (i) vegetative dry matter (VegDM), comprised of stems and
141 leaves, weighed after drying at 80°C for 48 h; (ii) spike length (SpL) (cm) measured from the
142 base of the spike to the start of awns at maturity stage; (iii and iv) flag leaf length (FLL) (cm)
143 and flag leaf width (FLW) (mm), of the longest and widest parts of the flag leaf, respectively.
144 Three representative plants were measured in each plot for each trait.

145 Three *derivative* sets of traits were obtained by calculating the deviations from the regression
146 line (residuals) that were then used for QTL mapping (Fig. 1). The first derivative set defined
147 here as ‘adjusted phenology traits’ was obtained, for each environment separately, by calculating
148 the residuals of linear regression between the means of the corresponding initial trait values and
149 DP-H values (Fig. 1, A) in order to exclude the effect of differences in flowering phenology on
150 these traits (prefix ‘df’ was added to the initial trait name):

$$151 \quad \hat{V}_{DH} = \beta + \alpha \cdot DH \quad (1)$$

$$152 \quad \varepsilon_{DH} = V - \hat{V}_{DH} \quad (2)$$

153 where: V is a value of the observed initial trait, DH is DP-H value, \hat{V}_{DH} is a predicted value

154 DH is DP-H value, \hat{V}_{DH} a predicted value of the trait based on linear regression, ε_{DH} is a

155 value of the trait based on linear regression, ε_{DH} is a residual from the regression line. The
156 regression line. The second derivative set defined here as ‘drought plasticity traits I’ was
157 obtained by calculating the residuals of linear regression between means of the initial trait values
158 in the WW and WL conditions (prefix ‘d’ was added to initial trait name), in order to get a
159 deviation between trait value in WL stress and WW condition, adjusted for the differences in
160 trait values in the population under normal conditions:

161
$$\hat{V}_{WL} = \beta + \alpha \quad (3)$$

162
$$\varepsilon_{WL} = V_{WL} - \hat{V}_{WL} \quad (4)$$

163 where: V_{WW} a value of the observed initial trait under WW conditions is a value of
164 conditions V_{WL} is a value of the observed initial trait under WL conditions, is a
165 conditions, \hat{V}_{WL} is a predicted value of the trait based on the linear regression, is a
166 regression, ε_{WL} is a residual from the regression line.

167 The third derivative set defined here as ‘drought plasticity traits II’ was obtained by calculating
168 the residuals of linear regression between means of the corresponding initial trait values in the
169 WL treatment and trait values in the WW conditions and DP-H values in the WL (prefix ‘ddf’
170 was added to the initial trait name), in order to exclude the effect of drought escape mechanisms
171 in ‘drought plasticity traits I’ by taking into account the effect of heading time:

172
$$\hat{V}_{WL}^{DH} = \beta + \alpha 1 \cdot V_{WW} - \alpha 2 \quad (5)$$

173
$$\varepsilon_{WL}^{DH} = V - \hat{V}_{WL}^{DH} \quad (6)$$

174 where: V_{WW} is a value of the observed initial trait under WW conditions, is a value of
175 conditions, V_{WL} is a value of the observed initial trait under WL conditions, is a
176 conditions, DH_{WL} is a value of DP-H under WL conditions, is a predicted value of the
177 \hat{V}_{WL} is a predicted value of the trait based on the linear regression, is a residual from the
178 ε_{WL} is a residual from the regression line.

179

180 **Statistical analysis of phenotypic data**

181 The JMP statistical package, version 11.0 (SAS Institute, Cary, NC, USA) was used for
182 correlation and regression analyses. Correlation network analysis was conducted with the
183 Software JASP 0.9 (JASP Team). Phenotypic values of initial and derivative traits were tested for
184 normal distribution. The analysis of variance (ANOVA) was performed as a factorial model,
185 with the irrigation regimes as fixed effects and genotypes and blocks as random effects.
186 Heritability (h^2) was calculated for each trait across the two irrigation treatments using variance
187 components of ANOVA:

$$188 \quad H^2 = \sigma_g^2 / (\sigma_g^2 + \sigma_{g \times e}^2 / e)$$

$$189 \quad \text{where: } \sigma_g^2 = [(MS_{gen} - MS_{gen \times e}) / e] \quad \sigma_{g \times e}^2 = MS_{gen \times e}$$

190 e is the number of environments and MS is the mean square. The correlation values and the
191 correlation values and the descriptive statistics were calculated on the mean values of phenotypic
192 data for each initial trait and corresponding derivative traits.

193 **Construction of high-density genetic map**

194 The genetic map was constructed using *MultiPoint* software, section «UltraDense»
195 (<http://www.multiqtl.com>) (Ronin *et al.*, 2017). After filtering for missing data (removing
196 markers with more than 10% missing data points) and large segregation distortion ($\chi^2 > 35$), the
197 function "bound together" was applied to select the best candidate skeleton markers representing
198 groups of co-segregating markers with size of ≥ 2). Clustering of candidate markers into linkage
199 groups (LG) was performed at the threshold of recombination fraction RF=0.2. The next step
200 included marker ordering and testing of the local map stability and monotonicity for each LG
201 (Mester *et al.*, 2003; Korol *et al.*, 2009). Reducing of the final number of LGs to 14,
202 corresponding to haploid number chromosomes of tetraploid wheat, was performed by merging
203 the LGs with minimum pairwise RF values expressed by their end markers (end-to-end
204 association). Orientation of each LG in relation to the short (S) and long (L) chromosome arms
205 was performed according to the correspondence of the mapped markers with those on the
206 consensus maps of hexaploid (Wang *et al.*, 2014) and tetraploid wheat (Maccafferri *et al.*, 2015).

207 **QTL analysis**

208 QTL analysis was performed using the general interval mapping (IM) procedure of MultiQTL
209 software package (<http://www.multiqtl.com>). First, single-QTL and two-linked-QTL models
210 were used for screening of genetic linkage for each trait in each environment separately (Korol *et*
211 *al.*, 2009). Multi-environment analysis (MEA) was performed by joint analysis of trait values
212 scored in two environments (WL and WW). After separate analysis for each chromosome,
213 multiple interval mapping (MIM) was used for reducing the residual variation for each QTL
214 under consideration, by taking into account QTLs that reside on other chromosomes (Kao *et al.*,
215 1999). The significance of the detected QTL effects was tested using 5000 permutation runs.
216 Significant models were further analyzed by 5000 bootstrap runs to estimate standard deviations
217 of the chromosomal position and QTL effect. Overlapping QTL effects, when a detected QTL
218 affects two or more separate traits, were referred to as multi-trait QTLs. The software MapChart
219 2.2 was used for visualization of the QTL map (Voorrips, 2002).

220 **Identification of physical position of the mapped SNP markers and CGs residing within** 221 **QTL intervals**

222 The physical positions of SNP markers were obtained by BLAST search of sequences of probes
223 (Wang *et al.*, 2014) against the whole-genome assembly of WEW accession ‘Zavitan’ (Avni *et*
224 *al.*, 2017). A list of genes residing within each QTL interval (1.5 LOD support interval of QTL
225 effect with highest LOD) was obtained from the annotated gene models of the ‘Zavitan’ genome
226 assembly (Avni *et al.*, 2017). The putative genetic positions of the potential CGs on the QTL
227 map were calculated based on a local linear approximation of genetic distances using the known
228 physical positions of CGs relative to near markers.

229 **Results**

230 **High-density genetic map**

231 Genotyping of the G×L RIL population, followed by quality control, resulted in 4,347
232 polymorphic SNP markers. Out of these, 4,015 SNPs representing 1,369 unique loci (skeleton
233 markers) were clustered into 14 LGs (Fig. S1). The genetic map covered 1835.7 cM (953.1 cM
234 for the A genome and 882.6 cM for the B genome) (Table S1-S2). The number of skeletal
235 markers and length of individual chromosome maps ranged from 51 (84.6 cM) for chr. 4B to 146
236 (165.3 cM) for chr. 5B. A relatively high proportion (6.3%) of non-recombinant chromosomes

237 was observed among $150 \times 14 = 2,100$ RIL \times chromosome combinations (Table S3). A total of 311
238 (22.7%) skeletal loci showed significant ($P \leq 0.05$) segregation distortion (Fig. S2), more
239 frequently in favor of the wild rather than domesticated parent allele (203 vs. 108, respectively).
240 The order of markers on the current genetic map showed highly similar positions on the WEW
241 pseudomolecules (average rank correlation coefficient 0.999) (Table S4).

242 **Relationships between phenotypic traits**

243 Normal distribution of most of the initial (excluding LR) and derivative quantitative traits of the
244 RIL population was observed in each of the two environments (Fig. S3-S5, Table S5). Most of
245 the initial and dftraits showed a wider distribution under WW than under WL conditions (Table
246 S6). Similar range of variation in WW and WL treatments was observed for initial and dftraits of
247 HI, FLW, LR and OP. Both phenological traits (DP-H and DH-M) and Chl exhibited a wider
248 range under WL (Table S6). ANOVA showed highly significant effects ($P \leq 0.001$) of irrigation
249 regimes for most of the traits (Table S7), except SpL and FLL ($0.01 \leq P \leq 0.05$). Genotype effect was
250 highly significant ($P \leq 0.001$) for most of the traits, except for VegDM and TotDM
251 ($0.001 < P < 0.01$) (Table S7). The irrigation \times genotype interaction was found to be significant
252 only for DH-M and KNSP.

253 Correlation analysis was performed for the four groups of data: initial traits, traits adjusted for
254 phenology, and drought plasticity traits I and II (with and without adjustment for phenology)
255 (Tables S8-S10, Fig.2). The strongest negative correlation was observed between two initial
256 phenological traits, DP-H and DH-M: -0.93 in WL and -0.46 in WW. Positive correlations were
257 observed between the initial yield related traits, biomass related traits, DH-M and CL in both
258 treatments. These traits showed negative correlation with DP-H under both conditions, with
259 stronger correlation in the WL. This trade-off between developmental periods from planting to
260 heading (DP-H) and from heading to maturity (DH-M) indicates strong interactions of these two
261 phenology related traits with most of the other traits. The relationships between morphological
262 traits and yield/biomass related traits showed varied patterns in different treatments. For
263 example, CL and FLW showed positive correlation with VegDM in the WW (0.29 and 0.28,
264 respectively), but no correlation in the WL. FLL and CL showed opposite directions of
265 correlation in WW and WL (0.29 and -0.20, respectively). Most of the physiological traits were
266 poorly correlated with traits of the other groups. All initial traits under WW were positively

267 correlated with corresponding traits under WL (Table S11) with the lowest association for OP (r
268 = 0.18) and the strongest association for DP-H ($r = 0.85$). Interestingly, variations in the traits
269 between treatments had strong negative association with the values of traits under WW (Table
270 S11).

271 The correlations of the derivative traits showed common pattern with those of the initial traits,
272 with few exceptions (Tables S8-S10, Fig 2). Notably, no significant correlation of dDP-H with
273 most plasticity traits was found. However, dDH-M was positively associated with productivity
274 and yield related traits, confirming the importance of grain filling stage duration mainly in the
275 water-limited conditions. Rank correlations (Kendall's tau) between the initial and adjusted for
276 heading traits (Table S12) were stronger for traits obtained under WW conditions compared to
277 those obtained under WL conditions, suggesting that the influence of heading date to other traits
278 was stronger in WL conditions. Relationships between the initial traits and dftraits showed
279 common, for both WW and WL conditions, pattern. The ranks of genotypes for the dftraits were
280 slightly different from those of the initial traits when the initial traits were uncorrelated to
281 heading date, whereas for traits highly correlated with heading, the ranks of genotypes for
282 dftraits have considerably changed. For example, the rank correlation between DH-M and dfDH-
283 M in WL conditions was only 0.18, since DH-M highly correlated with heading date (-0.93). On
284 the contrary, rank correlations between initial and drought plasticity traits were lower for more
285 plastic to drought traits that showed lower correlations between initial traits in WW and WL
286 conditions (Table S12).

287 **Genomic dissection of initial and derivative traits**

288 QTL analysis was performed for 17 initial traits and 49 derived traits; among the derived traits,
289 16 resulted from adjustment for the effect of phenology and 33 are considered here as drought
290 plasticity traits. In total, we detected 291 significant QTL effects distributed among 79 putative
291 QT loci (Tables S13-S14, Figs. S6-S19), out of which 44 revealed a pleiotropic effect on two or
292 more traits and 35 affected only one trait (Table 1, Table S14 and Fig.3). About one third of the
293 79 mapped loci had QTL effects only on the initial (13) or derivative (15) traits, while the
294 majority of loci (51 out of 79) included QTL effects on both, initial and derivative traits (Tables
295 S13-S14 and Figs. S6-S19).

296 **Genomic architecture of the studied traits in relation to phenology (heading time)**

297 The presence/absence of QTL effects for derivative traits (dftraits) was used for classification of
298 QTLs as ‘plastic’ or ‘non-plastic’ with respect to variation in phenology (Table 1, Table S14,
299 Fig. 3). Most of the QTLs (45 out of 79) showed significant effects on both, initial and derivative
300 traits. For 28 of these 45 QTLs, both effects were rather similar (Table S14). Therefore, we
301 defined them as ‘non-plastic’ with respect to variation of heading date (Fig. 4). The group of
302 QTLs classified as ‘plastic’ comprise of the following categories: (i) 17 QTLs that showed
303 increased LOD scores and estimates of dfQTL effects after adjustment of the initial traits for
304 variation in heading time (Fig. 4); (ii) 11 dfQTLs that affected only the derivative traits (Fig. 4);
305 and (iii) 7 QTLs that displayed pleiotropic effects on additional traits only after correction for
306 heading time (Table S13). Most of these 11 dfQTLs had an effect on a single trait only,
307 excluding QTL 1A.3 that affected TKW, KNSP and OP. A total of 10 QTLs had effect on DP-H
308 and 6 other QTLs displayed full suppression of QTL effects after adjustment for heading time.
309 Those loci were marked as ‘associated’ with heading (Fig. 4).

310 **Genomic dissection of drought plasticity traits**

311 QTLs were defined as ‘non-plastic’ in relation to drought when significant effects were revealed
312 for the initial traits, while no effect for drought plasticity traits (‘dtraits’ and/or ‘ddftraits’) was
313 detected in the same QTL region. On the contrary, QTLs that affected only drought plasticity
314 traits without displaying significant effect on the initial traits or QTLs with co-localization of
315 effects on both initial and derivative traits were classified as ‘plastic’ (Table S14, Fig.4).
316 According to this approach, we have identified 33 QTLs with plastic drought effects on at least
317 one trait (Table 1, Table S14, Fig. 4): 9 QTLs for dtraits; 11 QTLs for ddftraits and 13 QTLs for
318 combinations of dtraits and ddftraits. These results highlight the importance of adjusting for the
319 effect of heading time in QTL mapping of plasticity to water availability and adaptation to
320 drought. Most of plastic QTL effects (33 out 49) were collocated with corresponding initial
321 traits, while 15 QTL effects presented 14 QTLs affected on drought plasticity traits only. A
322 major plastic QTL for response to drought, 7B.1, affected six dtraits (dGY, dTKW, dKNSP, dHI,
323 dSpDM, and dDH-M) with ITV allele contributed by G18-16. The highest number of plastic
324 QTLs (six) was found for HI.

325 A comparison of QTL effects for plasticity to drought conferred by the G18-16 and LDN ITV
326 alleles is presented in Table 2. In most cases, the ITV alleles for the plasticity QTL effects on the

327 yield related traits (GY, TKW, KNSP) contributed by G18-16. For HI and SpDM, the number
328 and PEV scores of plasticity QTL effects, were very similar for ITV alleles contributed by LDN
329 and G18-16 (Table 2), while ITV alleles for plasticity QTL effects on VegDM and TotDM were
330 provided mainly by LDN. Plasticity of morphological traits showed different origin of ITV
331 alleles: equal for LDN and G18-16 for SpL; higher for LDN alleles for CL; higher for LDN for
332 flag leaf length trait, but higher for G18-16 for flag leaf width trait. QTL analysis of plasticity of
333 two DATs ($\delta^{13}\text{C}$ and OP) showed that allele for higher adaptability originated from G18-16.
334 QTLs for plasticity of Chl had equal number of ITV of G18-16 and LDN alleles. Plasticity of LR
335 was associated with the ITV allele of LDN in the two detected QTLs, suggesting high
336 importance of LR plasticity for plant adaptation to water deficit in LDN, which has wider leaves
337 than G18-16.

338 **QTLs associated with drought resistance strategies**

339 We attempted to use QTL effects on four DATs in order to classify the QTLs in relation to
340 drought resistance strategies, considering that OP is associated with drought tolerance strategy,
341 $\delta^{13}\text{C}$ and LR with avoidance strategy, and chlorophyll content as an indicator of the extent of
342 photosynthetic apparatus damage caused by the water-deficit stress. A total of 33 QTLs fell into
343 these categories, out of which 17 were designated as plastic (Table 3). Nevertheless, most of
344 these QTLs (67%) did not affect yield related traits. The ITV alleles for most of QTLs affecting
345 initial and plasticity DATs originated from G18-16 (79% and 65%, respectively). Four major
346 plastic drought QTLs were associated with drought avoidance: three for $\delta^{13}\text{C}$ (3A-1, 4A-3 and
347 7B-2 with G18-16 ITV allele) and one for LR (7A-4 with LDN ITV allele) (Table S13-S14). A
348 major QTL effect on OP was identified on chromosome 4B (QTL 4B-5) with the G18-16 allele
349 associated with drought tolerance (lower OP values). This QTL had also strong effect on FLW
350 with LDN ITV allele (Table S13-S14). In the current study, we have classified QTLs as
351 ‘drought-escape’ QTLs if they showed significant effects on drought plasticity I (dtraits), but no
352 effect on the corresponding ddftraits for drought plasticity II, (Table 3, Fig. 4).

353 **Candidate gene analysis**

354 More than 95% of SNPs (3824/4015) from our G×L genetic map were anchored to the reference
355 genome of tetraploid WEW (Avni *et al.*, 2017) (Table S2). The physical and genetic positions of
356 these SNP markers (Table S2) enabled us to define the physical intervals of QTLs and the

357 contents of genes within these intervals (Table S15). The physical intervals of QTLs ranged from
358 3.15 to 487.85 Mbp and the number of genes within these intervals varied from 25 to 2136
359 (Table S16). Most of QTLs with large intervals (>100 Mbp) were located in pericentromeric
360 regions. On the contrary, 16 QTLs with small physical intervals (<10 Mbp) and relatively low
361 gene content (Table S16) were dispersed along different chromosome parts, except for the
362 pericentromeric regions. Most of QTLs with more than 200 genes within intervals were excluded
363 from CG analysis. Our search for CGs was focused on known genes associated with studied
364 traits, regulation of flowering and development (genes related to hormonal pathways and
365 biosynthesis). We identified 53 potential CGs within our QTL intervals (Table S17). The
366 putative genetic positions of CGs on the QTL map are shown in Figs. S6-S19. The list the
367 candidates includes six CGs with well-known effect on the studied traits, *Glu-B3* (TKW),
368 *TaCly1* (SpL), *Wx-B1* (GY), *Wx-A1* (TKW), *WAP2-B* (SpL) and *Gpc-B1* (DH-M, TKW). A total
369 of 11 CGs related to phenology were identified within 8 QTL intervals (Table S17). Around half
370 of all CGs (26) were associated with regulation of hormonal balance: 13 CGs of them were
371 related to gibberellin (GA) signaling and biosynthesis and identified within eight QTL intervals
372 (Table S17), 11 CGs of them were associated with the ethylene signaling pathway and located
373 within ten QTLs, and two CGs of them were associated with regulation of auxin and found
374 within two QTLs. In addition, we identified two heat stress associated CGs (*HSFA2C* and
375 *HSP22.0*) within two QTLs, three genes related to transport of nitrate (*NRT2.6*) and sugars
376 (*STP1* and *SUT4*) within two QTLs affecting TKW, and a cluster of seven CGs with NAC
377 domain within interval of QTL 2A.7 affecting chlorophyll content.

378

379 **Discussion**

380 Phenotypic plasticity is one of the main mechanisms of adaptation to abiotic stresses via changes
381 in critical developmental stages, such as the timing of transition from vegetative to reproductive
382 growth (Kamran *et al.*, 2014; Riboni *et al.*, 2014). Altering flowering time is an evolutionary
383 strategy adopted by plants to cope with environmental stresses, such as drought, in order to
384 ensure maximum reproduction under changing environment (e.g. Kazan and Lyons, 2016).
385 However, the genetic diversity of many crops was eroded during domestication and subsequent
386 improvement under domestication, due to the one-sided selection for increasing of yield that

387 reduced adaptability of cultivars (Matesanz and Milla, 2018). The present study of genomic
388 architecture of agronomic and physiological traits plasticity in response to drought is
389 demonstrating the effect of heading time on adaptation to water limited conditions. The
390 comprehensive genetic analysis of the initial traits and their derivatives, based on regression
391 residuals, enabled to identify plasticity QTLs and tentatively classify them into several drought
392 adaptation strategies.

393 **Detection of QTLs using a high-density SNP-based genetic map**

394 Several QTL mapping studies were previously conducted based on a genetic map constructed by
395 genotyping of the G×L RIL population with SSR and DArT markers (Peleg *et al.*, 2008). These
396 studies included the genetic dissection of drought resistance (Peleg *et al.*, 2009a), grain protein
397 content (GPC) and grain micronutrient content (Peleg *et al.*, 2009b), and domestication related
398 traits (Peleg *et al.*, 2011; Tzarfati *et al.*, 2014). Genotyping of this RIL population with a high-
399 throughput SNP array allowed us to achieve a shorter map (1836 cM for SNPs vs. 2317 cM of
400 SSR-DArT map) and considerably increase the number of ordered polymorphic markers. Our
401 current map includes over four-fold higher amount of skeletal (framework) markers (1,369 vs.
402 307 in previous map) and five-fold smaller average interval lengths between adjacent markers
403 (1.3 cM vs.7.5 cM). In the current SNP map, the short arms of chromosomes 3A, 4A, 5A, 5B and
404 7A are extended and the short arm of chromosome 4B is fully present, while it was completely
405 absent in the previous map. Our results confirmed the observed earlier patterns of an increased
406 amount of non-recombinant chromosomes and segregation distortions for different chromosomes
407 in this population (Peleg *et al.*, 2008). The current SNP-based map allowed us to identify new
408 QTLs, with improved overlap of QTL effects and shorter QTL intervals. For example, on
409 chromosome 7AS we detected two linked QTLs affecting biomass related traits, first distal QTL
410 (7A.1) had effects with ITV allele of LDN and second QTL (7A.3) had ITV allele of G18-16 for
411 SpDM. The second QTL was previously detected (Peleg *et al.*, 2009), the corresponding
412 genomic region from G18-16 was introgressed into hexaploid cultivars (Merchuk-Ovnat *et al.*,
413 2016a, 2016b, 2017) and showed an improved GY and biomass under a range of water regimes
414 including water-deficit.

415 **Complexity of quantitative trait genetic architecture and the interaction with altered** 416 **phenology**

417 Correlation analysis and obtained results of QTL analysis clearly demonstrate the complexity of
418 the studied traits and their intra- and inter-group relationships. For example, all of the detected
419 QTLs for GY, SpDM, TotDM, SpL and DP-H traits conferred pleiotropic effects on other traits
420 and did not show even one case of a single-trait-only QTL effect. Moreover, the average
421 proportion of single-trait QTLs for the remaining 12 traits was also very low (~20%). Three
422 major QTLs (2B.6 and 7B.1, and 5A.3) for phenological traits, showed strong pleiotropic effects
423 on many other traits, with trade-off relationships between them. Furthermore, these effects were
424 considerably stronger under WL conditions. Similar trade-off related to the influence of
425 phenology was found in collection of Old World lupines (Berger *et al.*, 2017). Strong association
426 of phenology and other traits in genotypic (pleiotropic effects) and phenotypic (correlation)
427 levels, together with wide range of heading dates in the studied population, required taking
428 special measures to avoid potential biases in QTL analysis. Our results show that regression
429 analysis used for adjustment to heading date, enabled to increase the QTL detection power and
430 identify the relationships between the mapped QTLs and phenology.

431 **Drought-plasticity and drought-resistance strategies**

432 A variance ratio and a slope of norm reaction serve as two main methods of the phenotypic
433 plasticity quantification (Sadras and Richards, 2014). However, our approach can be applied as
434 an alternative to these methods with two advantages: (i) normalization of drought plasticity
435 scores for variation in the trait under non-stress conditions, (ii) accounting of the variation in
436 additional important factors, for example phenology. Linear regression residuals were previously
437 used for various purposes in the analysis of quantitative variation, such as the exclusion of the
438 effect of phenology on performance of pearl millet cultivars under drought conditions (Bidinger
439 *et al.*, 1983) and characterization of the impact of heat, corrected for differences in size of the
440 siliques between *Arabidopsis* accessions in control conditions (Bac-Molenaar *et al.*, 2016).
441 Nevertheless, it seems that the current study is the first to apply this approach for taking into
442 account differences in phenology in order to reduce biases in mapping plasticity QTL. Tétard-
443 Jones *et al.* (2011) used the reaction norm as a measure for plasticity traits to identify QTLs
444 associated with barley performance in response to aphids and rhizobacteria. Although we used a
445 different approach to map plasticity QTLs, we also found co-localization of QTL effects for the
446 initial and the plasticity traits, as well as the presence of separate QTLs affecting only plasticity

447 traits similar to the findings by Tétard-Jones *et al.* (2011). This phenomenon may have resulted
448 from pleiotropic and/or epistatic effects in the genetic control of phenotypic plasticity (Scheiner,
449 1993). Moreover, Gulisijia and Plotkin (2017) suggested that co-located effects are the result of
450 clustering of genes affecting phenotypic plasticity.

451 Three main strategies of drought resistance are recognized: drought escape, drought avoidance,
452 and drought tolerance (Levitt, 1980) and some authors recently proposed chlorophyll content as
453 an important drought adaptive trait (Guo and Gan, 2012; Tian *et al.*, 2013; Thomas and Ougham,
454 2014, Borrel *et al.*, 2014). Our results suggest that drought escape strategy played a central role
455 in wheat genetic adaptation to water stress especially in the Mediterranean region (Turner, 2004).

456 **Candidate genes within QTL intervals**

457 When full genome sequence is available, high-density genetic maps can provide sufficient
458 accuracy and resolution for the identification of CGs underlying the QTLs (Thudi *et al.*, 2014;
459 Mwadzingeni *et al.*; 2016a, Zhang *et al.*, 2017). For example, genes involved in flowering
460 pathways in cereals were proposed as CGs for QTLs associated with complex traits (Milner *et*
461 *al.*, 2016). In the current study, eight genes regulating flowering time were localized within 6 out
462 of 13 QTL intervals affecting phenology. Although, we did not identify major photoperiodic
463 wheat *Ppd* genes within these intervals, *Ppd-A1* (Beales *et al.*, 2007) was found within a QTL
464 interval on chromosome 2A affecting all biomass related traits as well as GY and KNSP after
465 adjustment for flowering time. Furthermore, the *TaGI*, which is known to be associated with
466 circadian clock regulation of photoperiodic response in wheat (Zhao *et al.*, 2005), was localized
467 together with *TaFT2-A* within the 3A.2 QTL interval for DP-H. The vernalization gene *Vrn-A1*
468 was localized within the interval of QTL 5A.5 affecting DP-H. Genes of *FT* family, which are
469 involved in regulation of flowering, development and plant adaptation (Halliwell *et al.*, 2016),
470 were localized within 4 QTL intervals, which affected phenological traits.

471 Crosstalk of plant hormones is involved in plant development and its response to abiotic stresses
472 (Peleg and Blumwald, 2011; Colenbrook *et al.*, 2014). GA biosynthesis genes and signaling
473 related genes are dispersed along several wheat chromosomes (Pearce *et al.*, 2015) and some of
474 them were proposed to be involved in response to abiotic stresses (e.g. Krugman *et al.*, 2011;
475 Colebrook *et al.*, 2014; Shu *et al.*, 2018). Our suggested CGs are in agreement with known
476 function of *GA2ox* genes in response to drought (Colebrook *et al.*, 2014) and our previous results

477 that showed differential expression of *GA2ox3* in response to drought for WEW accessions
478 (Krugman *et al.*, 2011). *Ga20ox* and *GASA* family genes are also known to be involved in
479 growth promotion under stress conditions (Peleg *et al.*, 2011; Colebrook *et al.*, 2014), while
480 *GAI3ox* genes were not reported previously as regulators of response to abiotic stresses.
481 Ethylene response factors are also involved in regulation of plant growth (Dubois *et al.*, 2018)
482 and stress responses (Dey and Vlot, 2015). Interestingly, these ethylene CGs were identified
483 within seven plastic to drought QTLs that highlights importance of this gene family for drought
484 resistance in wheat.

485 ***Vrn-B3* is a candidate gene for major drought escape QTL**

486 The 7B.1 QTL with the highest effect on DP-H explained 37% of the variation in flowering time.
487 The wild parent allele of 7B.1, associated with earlier heading in both, WW and WL,
488 prolongation of maturity period, and increasing of yield related traits in WL, appeared to have
489 strong effects on the plasticity of yield related traits. The *Vrn-B3* (*TaFT1*), known to affect
490 flowering in wheat (Yan *et al.*, 2006) and found to reside within this region (together with other
491 25 genes), seems to be a CG for these strong effects. This gene is a homologous to the
492 *FLOWERING LOCUS T* (*FT*) gene of Arabidopsis that plays a central role in control of
493 transition from vegetative to reproductive phase in flowering plants (Lv *et al.*, 2014). In barley
494 earlier flowering was associated with increasing of *HvFT1* copy number or with haplotype
495 differences in the promoter region and first intron of this gene (Nitcher *et al.*, 2013). Orthologs
496 of *FT* in different plant species were associated with regulation of flowering in response to
497 abiotic stresses (Pin and Nelson, 2012; Galbiati *et al.*, 2016); however, *TaFT1* was not reported
498 as a flowering regulator in response to drought in wheat previously.

499 **Conclusions and future perspectives**

500 Global climate changes require a better understanding of the genetic basis of crop plasticity in
501 response to drought and other abiotic stresses. Here we propose a new approach for
502 quantification of plasticity of complex traits measured under contrasting environmental
503 conditions, which can be utilized in classical QTL and GWAS analyses of plant response to a
504 wide range of biotic and abiotic stresses. Furthermore, application of the simultaneous
505 adjustment of drought plasticity and phenological differences in mapping population can
506 improve the accuracy of QTL mapping and reveal hidden during standard analysis plasticity

507 QTLs. The identification of CGs within QTL intervals may lead to the discovery of new
508 pleiotropic effects of these genes by their interactions with additional networks that affect not
509 only developmental processes, but also plant response to environmental stresses. For example,
510 *Vrn-B3* (*TaFT1*), which is proposed here as a CG underlying a major drought plasticity QTL,
511 possibly responsible for accelerated development of plants and significant improvement of yield
512 under WL conditions by the drought escape strategy. In addition, the higher phenotypic plasticity
513 of the WEW parental line is confirming the importance of crop wild relatives' gene pool for
514 improvement of crop adaptability to environmental stresses.

515 **Supplementary data**

516 Table S1 Summary of the genetic map constructed based on G×L RIL population.

517 Table S2 Genetic and physical positions of mapped SNPs.

518 Table S3 Number of RILs with parental (non-recombinant) chromosomes.

519 Table S4 Rank correlations of genetic positions of the mapped markers with corresponding
520 positions on other wheat genetic maps and physical positions and WEW genome assembly.

521 Table S5 Normality test of initial and derivative traits.

522 Table S6 Mean values and ranges of 17 phenotypic traits.

523 Table S7 Analyses of variance (Anova) and heritability (h^2).

524 Table S8 Association between 17 initial traits in both treatments.

525 Table S9 Associations between adjusted traits to time of heading in both treatments.

526 Table S10 Association between plasticity traits to water stress with and without accounting of
527 time of heading.

528 Table S11 Association between corresponding traits in WW and WL and their variation between
529 treatments.

530 Table S12 Kendall's tau coefficients of rank correlations between initial and derivative traits.

531 Table S13 Parameters of QTL effects.

532 Table S14 Summary of QTLs.

533 Table S15 List of HC genes within QTL intervals.

534 Table S16 Number of HC genes and physical intervals of QTLs.

535 Table S17 Summary of CGs.

536 Fig. S1 Distribution of attached markers along 14 wheat chromosomes.

537 Fig. S2 Segregation distortion for each chromosome in the G×L RIL population.

538 Fig. S3 Frequency distribution of the 150 F6 RILs for 17 initial phenotypic traits.

539 Fig. S4 Frequency distribution of the 150 F6 RILs for 16 adjusted for heading date traits.

540 Fig. S5 Frequency distribution of the 150 F6 RILs for 33 drought plasticity traits.

541 Fig. S6-S19 LOD score plot with putative genetic positions of CG and 1.5 LOD support intervals
542 of QTL effects for 14 chromosomes.

543 **Acknowledgements**

544 The research leading to these results has received funding from the European Community's
545 Seventh Framework Programme (FP7/ 2007-2013) under the grant agreement n°FP7- 613556,
546 Whealbi project; the Israeli Ministry of Agriculture and Rural Development, Chief Scientist
547 Foundation (Grants 837-0079-10 and 837-0162-14); the German Federal Ministry of Food and
548 Agriculture (FKZ: 2813IL03); the US-Israel Binational Agricultural Research and Development
549 Fund (US-4916-16); and ISF grant for equipment (grant no. 2289/16). We thank Andy Phillips
550 for his help with GA related genes, and Vered Barak for excellent technical assistance.

References

- Adiredjo AL, Navaud O, Muños S, Langlade NB, Lamaze T, Grieu P.** 2014. Genetic control of water use efficiency and leaf carbon isotope discrimination in sunflower (*Helianthus annuus* L.) subjected to two drought scenarios. *PLoS ONE* **9**, e101218.
- Ahmad MQ, Khan SH, Khan AS, Kazi AM, Basra S.** 2014. Identification of QTLs for drought tolerance traits on wheat chromosome 2A using association mapping. *International Journal of Agriculture and Biology* **16**, 862–870.
- Avni R, Nave M, Barad O, Baruch K, Twardziok SO, Gundlach H, Hale I, Mascher M, Spannagl M, Wiebe K et al.** 2017. Wild emmer genome architecture and diversity elucidate wheat evolution and domestication. *Science* **357**, 93–97.
- Bac-Molenaar JA, Fradin EF, Becker FFM, Rienstra JA, van der Schoot J, Vreugdenhil D, Keurentjes JJB.** 2015. Genome-wide association mapping of fertility reduction upon heat stress reveals developmental stage-specific QTLs in *Arabidopsis thaliana*. *Plant Cell* **27**, 1857–1874.
- Beales J, Turner A, Griffiths S, Snape JW, Laurie DA.** 2007. A *Pseudo-Response Regulator* is misexpressed in the photoperiod insensitive *Ppd-D1a* mutant of wheat (*Triticum aestivum* L.). *Theoretical and Applied Genetics* **115**, 721–733.
- Berger J, Shrestha D, Ludwig C.** 2017. Reproductive strategies in Mediterranean legumes: Trade-offs between phenology, seed size and vigor within and between wild and domesticated *Lupinus* species collected along aridity gradients. *Frontiers in Plant Science* **8**, 548.
- Bidinger FR, Mahalakshmi Y, Talukdar BS, Alagarswamy G.** 1982. Improvement of drought resistance in pearl millet. In: IRRI, eds. *Drought resistance in crops with emphasis on rice*. Los Banos, Philippines: IRRI, 357–375.
- Bloomfield JA, Rose TJ, King GJ.** 2014. Sustainable harvest: managing plasticity for resilient crops. *Plant Biotechnology Journal* **12**, 517–533.
- Blum A.** 2011. Drought resistance – is it really a complex trait? *Functional Plant Biology* **38**, 753–757.

Blum A. 2017. Osmotic adjustment is a prime drought stress adaptive engine in support of plant production. *Plant, Cell & Environment* **40**, 4–10.

Borrell AK, Mullet JE, George-Jaeggli B, van Oosterom EJ, Hammer GL, Klein PE, Jordan DR. 2014. Drought adaptation of stay-green sorghum is associated with canopy development, leaf anatomy, root growth, and water uptake. *Journal of Experimental Botany* **65**, 6251–6263.

Colebrook EH, Thomas SG, Phillips AL, Hedden P. 2014. The role of gibberellin signalling in plant responses to abiotic stress. *Journal of Experimental Biology* **217**, 67–75.

Dey S, Corina Vlot A. 2015. Ethylene responsive factors in the orchestration of stress responses in monocotyledonous plants. *Frontiers in Plant Science*. **6**, 640.

Doyle J. 1991. DNA protocols for plants. In: Hewitt GM, Johnston AWB, Young JPW, eds. *Molecular techniques in taxonomy. NATO ASI Series (Series H: Cell Biology)* **57**. Berlin, Germany: Springer, 283–293.

Dubois M, Van den Broeck L, Inze D. 2018. The pivotal role of ethylene in plant growth. *Trends in Plant Science* **23**, 311–323.

Fuller D.Q. 2007. Contrasting patterns in crop domestication and domestication rates: recent archaeobotanical insights from the Old World. *Annals of Botany* **100**, 903–924.

Galbiati F, Chiozzotto R, Locatelli F, Spada A, Genga A, Fornara F. 2016. *Hd3a*, *RFT1* and *Ehd1* integrate photoperiodic and drought stress signals to delay the floral transition in rice. *Plant, Cell & Environment* **39**, 1982–1993.

Graziani M, Maccaferri M, Royo C, Salvatorelli F, Tuberosa R. 2014. QTL dissection of yield components and morpho-physiological traits in a durum wheat elite population tested in contrasting thermo-pluviometric conditions. *Crop & Pasture Science* **65**, 80–95.

Gulisija D, Plotkin JB. 2017. Phenotypic plasticity promotes recombination and gene clustering in periodic environments. *Nature Communications* **8**, 2041.

Guo Y, Gan S. 2012. Convergence and divergence in gene expression profiles induced by leaf senescence and 27 senescence-promoting hormonal, pathological and environmental stress treatments. *Plant, Cell & Environment* **35**, 644–655.

Halliwell J, Borrill P, Gordon A, Kowalczyk R, Pagano ML, Saccomanno B, Bentley AR, Uauy C, Cockram J, Bentley AR. 2016. Systematic investigation of FLOWERING LOCUS T-like poaceae gene families identifies the short-day expressed flowering pathway gene, *TaFT3* in wheat (*Triticum aestivum* L.). *Frontiers in Plant Science* **7**, 857.

Hedden P, Sponsel V. 2015. A century of gibberellin research. *Journal of Plant Growth Regulation* **34**, 740–760.

Henry RJ, Nevo E. 2014. Exploring natural selection to guide breeding for agriculture. *Plant Biotechnology Journal* **12**, 655–662.

Herzig P, Maurer A, Draba V, Sharma R, Draicchio F, Bull H, Milne L, Thomas TBW, Flavell AJ, Pillen K. 2018. Contrasting genetic regulation of plant development in wild barley grown in two European environments revealed by nested association mapping. *Journal of Experimental Botany* **7**, 1517–1531.

Hill CB, Taylor JD, Edwards J, Mather D, Bacic A, Langridge P, Roessner U. 2013. Whole-genome mapping of agronomic and metabolic traits to identify novel quantitative trait loci in bread wheat grown in a water-limited environment. *Plant Physiology* **162**, 1266–1281.

Huang L, Raats D, Sela H, Klymiuk V, Lidzbarsky G, Feng L, Krugman T, Fahima T. 2016. Evolution and adaptation of wild emmer wheat populations to biotic and abiotic stresses. *Annual Review of Phytopathology* **54**, 279–301.

Kamran A, Iqbal M, Spaner D. 2014. Flowering time in wheat (*Triticum aestivum* L.): a key factor for global adaptability. *Euphytica* **197**, 1–26.

Kao CH, Zeng ZB, Teasdale R.D. 1999. Multiple interval mapping for quantitative trait loci. *Genetics* **152**, 1203–1216.

Kazan K, Lyons R. 2016. The link between flowering time and stress tolerance. *Journal of Experimental Botany* **67**, 47–60.

Korol AB, Mester D, Frenkel Z, Ronin YI. 2009. Methods for genetic analysis in the Triticeae. In Feuillet C, Muehlbauer GJ, eds. *Genetics and genomics of the Triticeae. Plant Genetics and Genomics: Crops and Models* **7**. New York, USA: Springer + Business Media LLC, 163–199.

Kosina P, Reynolds M, Dixon J, Joshi A. 2007. Stakeholder perception of wheat production constraints, capacity building needs, and research partnerships in developing countries. *Euphytica* **157**, 475–483.

Krugman T, Chagué V, Peleg Z, Balzergue S, Just J, Korol AB, Nevo E, Saranga Y, Chalhoub B, Fahima T. 2010. Multilevel regulation and signalling processes associated with adaptation to terminal drought in wild emmer wheat. *Functional & Integrative Genomics* **10**, 167–186.

Krugman T, Peleg Z, Quansah L, Chagué V, Korol AB, Nevo E, Saranga Y, Fait A, Chalhoub B, Fahima T. 2011. Alteration in expression of hormone-related genes in wild emmer wheat roots associated with drought adaptation mechanisms. *Functional & Integrative Genomics* **11**, 565–583.

Lacaze X, Hayes PM, Korol A. 2009. Genetics of phenotypic plasticity: QTL analysis in barley, *Hordeum vulgare*. *Heredity* **102**, 163–173.

Leng G, Tang Q, Rayburg S. 2015. Climate change impacts on meteorological, agricultural and hydrological droughts in China. *Global and Planetary Change* **126**, 23–34.

Levitt J. 1980. *Responses of plants to environmental stresses*. New York, USA: Academic Press.

Levy AA, Feldman M. 1987. Increase in grain protein percentage in high-yielding common wheat breeding lines by genes from wild tetraploid wheat. *Euphytica* **36**, 353–359.

Lopes M, Dreisigacker S, Peña R, Sukumaran S, Reynolds M. 2014a. Genetic characterization of the Wheat Association Mapping Initiative (WAMI) panel for dissection of complex traits in spring wheat. *Theoretical and Applied Genetics* **128**, 453–464.

Lopes MS, Rebetzke GJ, Reynolds M. 2014b. Integration of phenotyping and genetic platforms for a better understanding of wheat performance under drought. *Journal of Experimental Botany* **65**, 6167–6177.

Lv B, Nitcher R, Han X, Wang S, Ni F, Li K, Pearce S, Wu J, Dubcovsky J, Fu D. 2014. Characterization of *FLOWERING LOCUS T1 (FT1)* gene in *Brachypodium* and wheat. *PLoS ONE* **9**, e94171.

Maccaferri M, Ricci A, Salvi S, Milner SG, Noli E, Martelli PL, Casadio R, Akhunov E, Scalabrin S, Vendramin V et al. 2014. A high-density, SNP-based consensus map of tetraploid wheat as a bridge to integrate durum and bread wheat genomics and breeding. *Plant Biotechnology Journal* **13**, 648–663.

Mann EM, Gleick HP. 2015. Climate change and California drought in the 21st century. *PNAS* **112**, 3858–3859.

Matesanz S, Milla R. 2018. Differential plasticity to water and nutrients between crops and their wild. *Environmental and Experimental Botany* **145**, 54–63.

Merchuk-Ovnat L, Barak V, Fahima T, Ordon F, Lidzbarsky GA, Krugman T, Saranga Y. 2016a. Ancestral QTL alleles from wild emmer wheat improve drought resistance and productivity in modern wheat cultivars. *Frontiers in Plant Science* **7**, 452.

Merchuk-Ovnat L, Fahima T, Krugman T, Saranga Y. 2016b. Ancestral QTL alleles from wild emmer wheat improve grain yield, biomass and photosynthesis across environments in modern wheat. *Plant Science* **251**, 23–34.

Merchuk-Ovnat L, Fahima T, Ephrath EJ, Krugman T, Saranga Y. 2017. Ancestral QTL alleles from wild emmer wheat enhance root development under drought in modern wheat. *Frontiers in Plant Science* **8**, 703–715.

Messmer R, Fracheboud Y, Bänziger M, Vargas M, Stamp P, Ribaut JM. 2009. Drought stress and tropical maize: QTL-by-environment interactions and stability of QTLs across environments for yield components and secondary traits. *Theoretical and Applied Genetics* **119**, 913–930

Mester D, Ronin Y, Minkov D, Nevo E, Korol A. 2003. Constructing large-scale genetic maps using an evolutionary strategy algorithm. *Genetics* **165**, 2269–2282.

Mickelbart MV, Hasegawa PM, Bailey-Serres J. 2015. Genetic mechanisms of abiotic stress tolerance that translate to crop yield stability. *Nature Reviews Genetics* **16**, 237–251.

Milner SG, Maccaferri M, Huang BE, Mantovani P, Massi A, Frascaroli E, Tuberosa R, Salvi S. 2016. A multiparental cross population for mapping QTL for agronomic traits in durum wheat (*Triticum turgidum* ssp. *durum*). *Plant Biotechnology Journal* **14**, 735–748.

Muqaddasi QH, Brassac J, Börner A, Pillen K, Röder MS. 2017. Genetic architecture of anther extrusion in spring and winter wheat. *Frontiers in Plant Science* **8**, 754.

Mwadzingeni L, Shimelis H, Dube E, Laing MD, Tsilo TJ. 2016a. Breeding wheat for drought tolerance: Progress and technologies. *Journal of Integrative Agriculture* **15**, 935–943.

Mwadzingeni L, Shimelis H, Tesfay S, Tsilo TJ. 2016b. Screening of bread wheat genotypes for drought tolerance using phenotypic and proline analyses. *Frontiers in Plant Science* **7**, 1276.

Nam WH, Hayes MJ, Svoboda MD, Tadesse T, Wilhite DA. 2015. Drought hazard assessment in the context of climate change for South Korea. *Agricultural Water Management* **160**, 106–117.

Nevo E, Korol AB, Bailes A, Fahima T. 2002. *Evolution of wild emmer and wheat improvement*. Berlin, Germany: Springer-Verlag.

Nicotra AB, Atkin OK, Bonser SP, Davidson AM, Finnegan EJ, Mathesius U, Poot P, Purugganan MD, Richards CL, Valladares F et al. 2010. Plant phenotypic plasticity in a changing climate. *Trends in Plant Science* **15**, 684–692.

Nitcher R, Distelfeld A, Tan C, Yan L, Dubcovsky J. 2013. Increased copy number at the *HvFT1* locus is associated with accelerated flowering time in barley. *Molecular Genetics and Genomics* **288**, 261–275.

Onogi A, Ideta O, Yoshioka T, Ebana K, Yamasaki M, Iwata H. 2016. Uncovering a nuisance influence of a phenological trait of plants using a nonlinear structural equation: application to days to heading and culm length in asian cultivated rice (*Oryza sativa* L.). *PLoS ONE* **11**, e0148609.

Pearce S, Huttly AK, Prosser IM, Li YD, Vaughan SP, Gallova B, Patil A, Coghill JA, Dubcovsky J, Hedden P et al. 2015. Heterologous expression and transcript analysis of gibberellin biosynthetic genes of grasses reveals novel functionality in the *GA3ox* family. *BMC Plant Biology* **15**, 130.

Peleg Z, Fahima T, Abbo S, Krugman T, Nevo E, Yakir D, Saranga Y. 2005. Genetic diversity for drought resistance in wild wheat and its ecogeographical association. *Plant, Cell & Environment* **28**, 176–191.

Peleg Z, Saranga Y, Suprunova T, Ronin Y, Röder M, Kilian A, Korol A, Fahima T. 2008. High-density genetic map of durum wheat × wild emmer wheat based on SSR and DArT markers. *Theoretical and Applied Genetics* **117**, 103–115.

Peleg Z, Fahima T, Krugman T, Abbo S, Yakir D, Korol AB, Saranga Y. 2009a. Genomic dissection of drought resistance in durum wheat × wild emmer wheat recombinant inbred line population. *Plant, Cell & Environment* **32**, 758–779.

Peleg Z, Cakmak I, Ozturk L, Yazici A, Jun Y, Budak H, Korol AB, Fahima T, Saranga Y. 2009b. Quantitative trait loci conferring grain mineral nutrient concentrations in durum wheat × wild emmer wheat RIL population. *Theoretical and Applied Genetics* **119**, 353–369.

Peleg Z, Blumwald E. 2011. Hormone balance and abiotic stress tolerance in crop plants. *Current Opinion in Plant Biology* **14**, 290–295.

Peleg Z, Fahima T, Korol AB, Abbo S, Saranga Y. 2011. Genetic analysis of wheat domestication and evolution under domestication. *Journal of Experimental Botany* **62**, 5051–5061.

Pin PA, Nilsson O. 2012. The multifaceted roles of FLOWERING LOCUS T in plant development. *Plant, Cell & Environment* **35**, 1742–1755.

Pinto RS, Reynolds MP, Mathews KL, McIntyre CL, Olivares-Villegas JJ, Chapman SC. 2010. Heat and drought adaptive QTL in a wheat population designed to minimize confounding agronomic effects. *Theoretical and Applied Genetics* **121**, 1001–1021.

Price AH, Cairns JE, Horton P, Jones HG, Griffiths H. 2002. Linking drought-resistance mechanisms to drought avoidance in upland rice using a QTL approach: progress and new opportunities to integrate stomatal and mesophyll responses. *Journal of Experimental Botany* **53**, 989–1004.

Rebetzke GJ, Condon AG, Farquhar GD, Appels R, Richards RA. 2008. Quantitative trait loci for carbon isotope discrimination are repeatable across environments and wheat mapping populations *Theoretical and Applied Genetics* **118**, 123–137.

Riboni M, Robustelli A, Galbiati M, Tonelli C, Conti L. 2016. ABA-dependent control of *GIGANTEA* signalling enables drought escape via up-regulation of *FLOWERING LOCUS T* in *Arabidopsis thaliana*. *Journal of Experimental Botany* **22**, 6309–6322.

Riboni M, Robustelli TA, Galbiati M, Tonelli C, Conti L. 2014. Environmental stress and flowering time: The photoperiodic connection. *Plant Signaling & Behavior* **9**, e29036.

Ronin YI, Mester DI, Minkov DG, Akhunov E, Korol AB. 2017. Building ultra-high-density linkage maps based on efficient filtering of trustable markers. *Genetics* **206**, 1285–1295.

Russo MA, Ficco DBM, Laido G, Marone D, Papa R, Blanco A, Gadaleta A, De Vita P, Mastrangelo AM. 2014. A dense durum wheat \times *T. dicoccum* linkage map based on SNP markers for the study of seed morphology. *Molecular Breeding* **34**, 1579–1597.

Sabadin PK, Malosetti M, Boer MP, Tardin FD, Santos FG, Guimaraes CT, Gomide RL, Andrade CL, Albuquerque PE, Caniato FF et al. 2012. Studying the genetic basis of drought tolerance in sorghum by managed stress trials and adjustments for phenological and plant height differences. *Theoretical and Applied Genetics* **124**, 1389–1402.

Scheiner SM. 1993. Genetics and evolution of phenotypic plasticity. *Annual Review of Ecology, Evolution, and Systematics* **24**, 35–68.

Shavrukov Y, Kurishbayev A, Jatayev S, Shvidchenko V, Zotova L, Koekemoer F, de Groot S, Soole K, Langridge P. 2017. Early flowering as a drought escape mechanism in plants: How can it aid wheat production? *Frontiers in plant science* **8**, 1950.

Shu K, Zhou W, Chen F, Luo X, Yang W. 2018. Abscisic acid and gibberellins antagonistically mediate plant development and abiotic stress responses. *Frontiers in Plant Science* **9**, 416.

Tardieu F, Tuberosa R. 2010. Dissection and modeling of abiotic stress tolerance in plants. *Current Opinion in Plant Biology* **13**, 206–212.

Tetard-Jones C, Kertesz MA, Preziosi RF. 2011. Quantitative Trait Loci mapping of phenotypic plasticity and genotype–environment interactions in plant and insect performance. *Philosophical Transactions of the Royal Society B: Biological Sciences* **366**, 1368–1379.

Tian F, Gong J, Zhang J, Zhang M, Wang G, Li A, Wang W. 2013. Enhanced stability of thylakoid membrane proteins and antioxidant competence contribute to drought stress resistance in the *tasg1* wheat stay-green mutant. *Journal of Experimental Botany* **64**, 1509–1520.

Thomas H, Ougham H. 2014. The stay-green trait. *Journal of Experimental Botany* **65**, 3889–3900.

Thudi M, Gaur PM, Krishnamurthy L, Mir RR, Kudapa H, Fikre A, Kimurto P, Tripathi S, Soren KR, Mulwa R et al. 2014. Genomics-assisted breeding for drought tolerance in chickpea. *Functional Plant Biology* **41**, 1178–1190.

Turner NC. 2004. Sustainable production of crops and pastures under drought in a Mediterranean environment. *Annals of Applied Biology* **144**, 139–147.

Tzarfati R, Saranga Y, Barak V, Gopher A, Korol AB, Abbo S. 2013. Threshing efficiency as an incentive for rapid domestication of emmer wheat. *Annals of Botany* **112**, 829–837.

Van Eeuwijk FA, Bink MCAM, Chenu K, Chapman SC. 2010. Detection and use of QTL for complex traits in multiple environments. *Current Opinion in Plant Biology* **13**, 193–205.

Voorrips RE. 2002. MapChart: software for the graphical presentation of linkage maps and QTLs. *Journal of Heredity* **93**, 77–78.

Wang S, Wong D, Forrest K, Allen A, Chao S, Huang BE, Maccaferri M, Salvi S, Milner SG, Cattivelli L et al. 2014. Characterization of polyploid wheat genomic diversity using a high-density 90 000 single nucleotide polymorphism array. *Plant Biotechnology Journal* **12**, 787–796.

Yan L, Loukoianov A, Blechl A, Tranquilli G, Ramakrishna W, SanMiguel P, Bennetzen JL, Echenique V, Dubcovsky J. 2004. The wheat *VRN2* gene is a flowering repressor down-regulated by vernalization. *Science* **303**, 1640–1644.

Yan L, Loukoianov A, Tranquilli G, Helguera M, Fahima T, Dubcovsky J. 2003. Positional cloning of the wheat vernalization gene *VRN1*. *PNAS USA* **100**, 6263–6268.

Yan L, Fu D, Li C, Blechl A, Tranquilli G, Bonafede M, Sanchez A, Valarik M, Yasuda S, Dubcovsky J. 2006. *The wheat and barley vernalization gene VRN3 is an orthologue of FT*. *PNAS USA* **103**, 19581–19586.

Zhang D, Zhang H, Chu S, Li H, Chi Y, Triebwasser-Freese D, Lv H, Yu D. 2017. Integrating QTL mapping and transcriptomics identifies candidate genes underlying QTLs associated with soybean tolerance to low-phosphorus stress. *Plant Molecular Biology* **93**, 137–50.

Zhao XY, Liu MS, Li JR, Guan CM, Zhang XS. 2005. The wheat *TaG11*, involved in photoperiodic flowering, encodes an Arabidopsis *GI* ortholog. *Plant Molecular Biology* **58**, 53–64.

.

Table 1 Summary of QTL effects associated with yield, biomass and phenology related, morphological, and drought adaptive physiological, traits, under water limited (WL) and well-watered (WW) conditions

Trait	# QTLs			LOD	ITV allele		Environmental specificity		Relation to phenology			Relation to drought	
	Total	Multi-trait	Single-trait		G18-16	LDN	WL	WW	Associated	Non-plastic	Plastic	Non-plastic	Plastic
<i>Yield related traits</i>													
GY	8	8	0	2.1-11.2	2	6	1	0	2	5	1	7	1
TKW	16	9	7	2.3-9.2	9	7	4	2	4	7	5	12	4
KNSP	11	10	1	2.3-8.9	2	9	1	0	4	4	3	9	2
HI	13	10	3	2.2-23.9	7	6	2	1	4	6	3	7	6
<i>Biomass related traits</i>													
SpDM	10	10	0	2.0-13.9	4	6	0	0	3	3	4	6	4
VegDM	6	5	1	2.2-4.4	1	4	0	0	0	4	1	1	4
TotDM	6	6	0	2.0-5.4	1	5	1	0	1	4	1	5	1
<i>Morphological traits</i>													
CL	15	12	3	2.5-9.5	4	11	0	1	6	3	6	10	5
SpL	10	10	0	2.0-10.8	6	4	1	1	2	4	4	7	3
FLL	9	7	2	2.0-7.7	3	6	0	0	4	3	2	6	3
FLW	17	13	4	2.1-32.4	8	9	0	2	5	10	2	14	3
<i>Drought adaptive physiological traits</i>													
δ13C	8	6	2	2.2-9.3	7	1	1	0	1	7	0	4	4
OP	9	7	2	2.3-4.9	1	8	0	3	0	6	3	7	2
Chl	13	10	3	2.0-7.0	7	6	0	2	1	5	7	11	2
LR	5	3	2	2.1-5.9	3	2	0	0	1	3	1	3	2
<i>Phenology related traits</i>													
DPH	10	8	2	2.4-40.8	3	7	0	0	10	0	0	5	5
DPM	8	8	0	3.0-13.6	4	4	1	0	5	2	1	6	2
All	78	44	34	2.0-40.8		--	--	--	15	41	21	46	33

Table 2 Number of QTL effects with ITV alleles of drought plasticity QTL effects, conferred by the G18-16 and LDN

Trait	ITV allele of LDN		ITV allele of G18-16	
	Number of QTLs	Total PEV*	Number of QTLs	Total PEV*
GY	0	0	1	0.21
TKW	1	0.13	3	0.37
KNSP	0	0	2	0.26
HI	3	0.33	3	0.39
SpDM	2	0.22	2	0.29
VegDM	3	0.31	1	0.13
TotDM	1	0.14	0	0
CL	4	0.46	1	0.11
SpL	2	0.17	1	0.17
FLL	2	0.21	1	0.14
FLW	1	0.12	2	0.21
$\delta^{13}C$	0	0	4	0.53
OP**	2	0.30	0	0
Chl	1	0.09	1	0.09
LR	2	0.24	0	0
DH-M	1	0.12	2	0.32

* Total PEV was calculated as a sum of PEV of effects of dtraits and ddtraits. When effects were co-located, PEV of higher effect was used for sum.

** Higher value of OP was associated with susceptibility to drought, allele contributed more negative values was associated with adaptivity.

Table 3 Summary of QTLs associated with drought resistance strategies and chlorophyll content.

Drought strategy	# QTLs	# QTLs plastic to drought	Allele responsible for drought resistance		Effect on productivity***		
			G18-16	LDN	-	0	+
Escape	4	4	2 (2)	2 (2)	0	0	4
Avoidance	13	5	10 (4)	3 (1)	2	9	2
Tolerance	9	3	8 (2)*	1 (1)	1	5	3
Chlorophyll content	13	5	7 (3)	6 (2)	0	8	5
Total	33**	17	26 (11)	11 (6)	3	22	13

* for osmotic potential lower value reflects higher drought tolerance

** the total number of QTLs presented in the column is lower than the sum of the number in the cells due to the fact that some of the QTLs had pleiotropic effects on traits associated with different drought strategies.

*** positive effect (+) means the same ITV allele for the effects of the QTL on yield related traits and physiological traits associated with drought resistance, while negative effect (-) means alternative ITV alleles; cases with no effect on productivity are denoted as '0'.

Number of plastic QTLs for each allele responsible for drought resistance were shown in brackets.

Figure legends

Fig. 1 Graphical representation of the regression approach for calculation of derivative traits. A) Linear regression was calculated between means of corresponding initial traits and days from planting to heading (DH) to get predicted values of trait (\hat{V}_{DH}). Obtained residuals between observed and predicted values of traits were used as “adjusted phenology traits” for each environment separately. B) Linear regression was calculated between means of the initial trait values in the WW and WL conditions (\hat{V}_{WL}) and linear regression between means of the corresponding initial trait values in the WL treatment and trait values in the WW conditions and DP-H values (DH) in the dry treatment (\hat{V}_{WL}^{DH}). Obtained residuals were used as “drought plasticity traits I” and “drought plasticity traits II”, respectively.

Fig. 2 Phenotypic relationships of the analyzed traits based on correlation network analysis in 150 RILs of G×L population. The correlations between traits are shown separately for WW and for WL treatments: (A) and (B) for initial traits; (C) and (D) for traits adjusted for the effect of phenology. Correlations within group of plasticity traits without and with adjustment for the effect of phenology are presented in (E) and (F), respectively. Green hexagons are representing group of yield related traits, blue squares – group of biomass related traits, pink rhombuses – group of morphology related traits, yellow circles – drought adaptive traits and red octagons – phenology related traits. Width of lines represents the strength of correlation (minimum level of correlation is 0.16), red and blue colors correspond to positive and negative association, respectively.

Fig. 3 Genetic architecture of 17 traits and their relationships with phenology and plasticity to drought stress. According to our classification, QTLs were marked as follows: non-plastic (NP); plastic (P) and associated to heading (A). With respect to drought resistance strategies the QTLs were marked as: escape (E); avoidance (A); tolerance (T); chlorophyll content (Ch) and ‘no associated strategy’ (N). The origin of ITV allele is indicated as G for G18-16 and L for LDN. QTL effects only on adjusted for phenology were marked by one asterisk (*), only on plasticity traits to drought with two asterisks (**). QTLs with effects on drought plasticity traits were marked by blue dash border.

Fig. 4 Examples of classification of detected QTLs in relation to phenology and drought plasticity: (a) non-plastic to phenology and drought QTL 6A.2; (b) plastic to phenology QTL 7A.2; (c) non-plastic to phenology and plastic to drought QTL 5A.2; (d) associated to phenology and related to drought escape strategy QTL 7B.1.

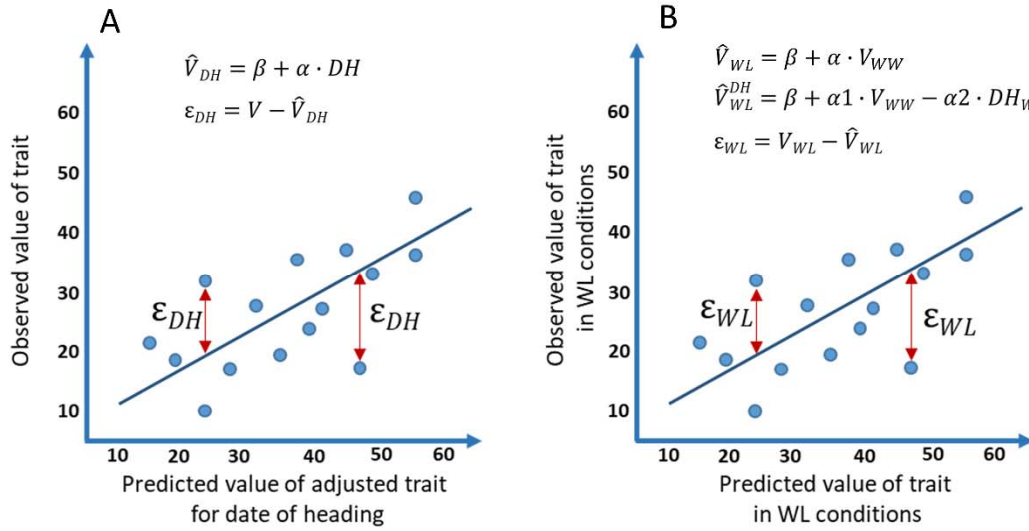


Fig. 1

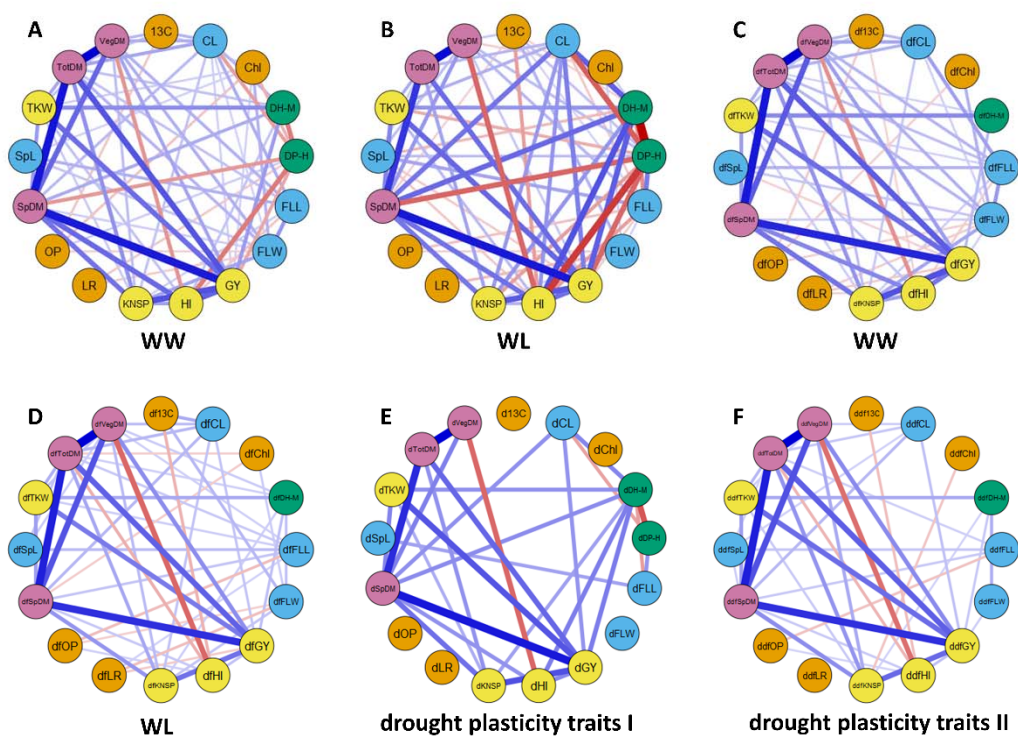


Fig. 2

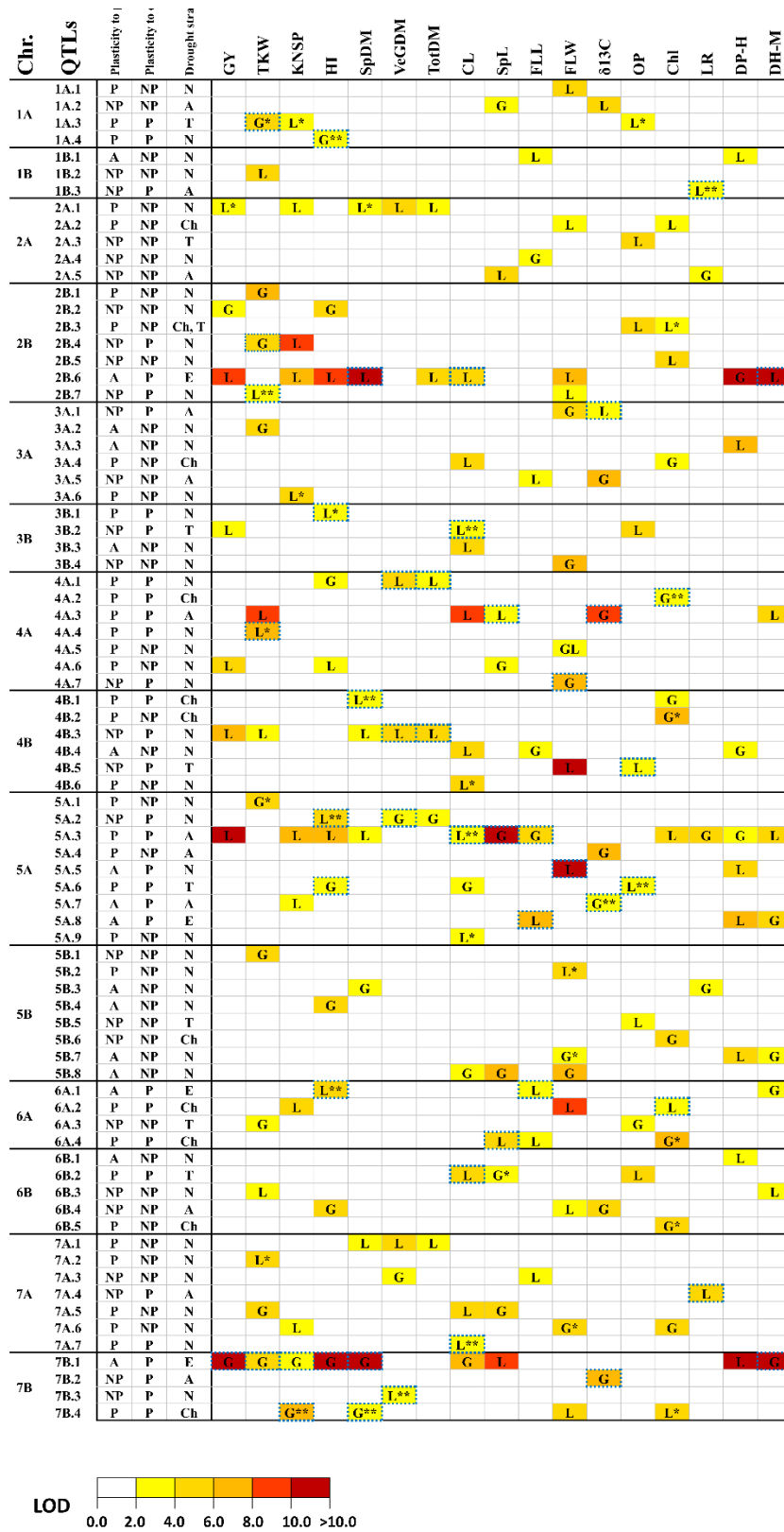


Fig. 3

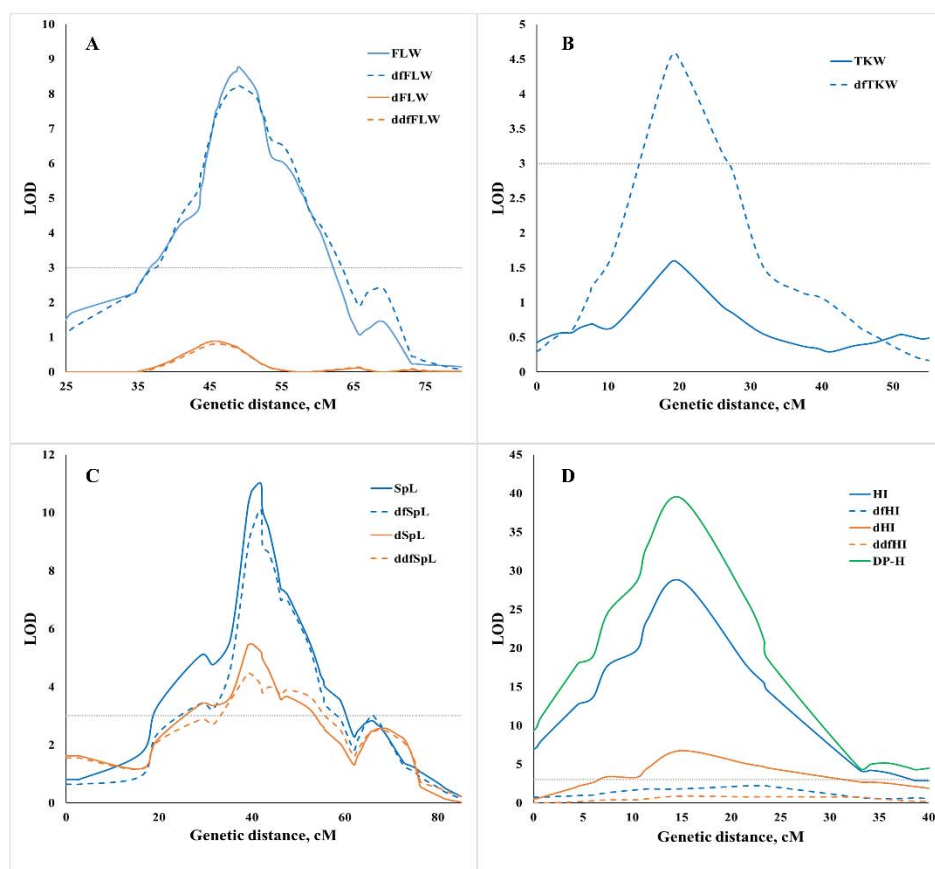
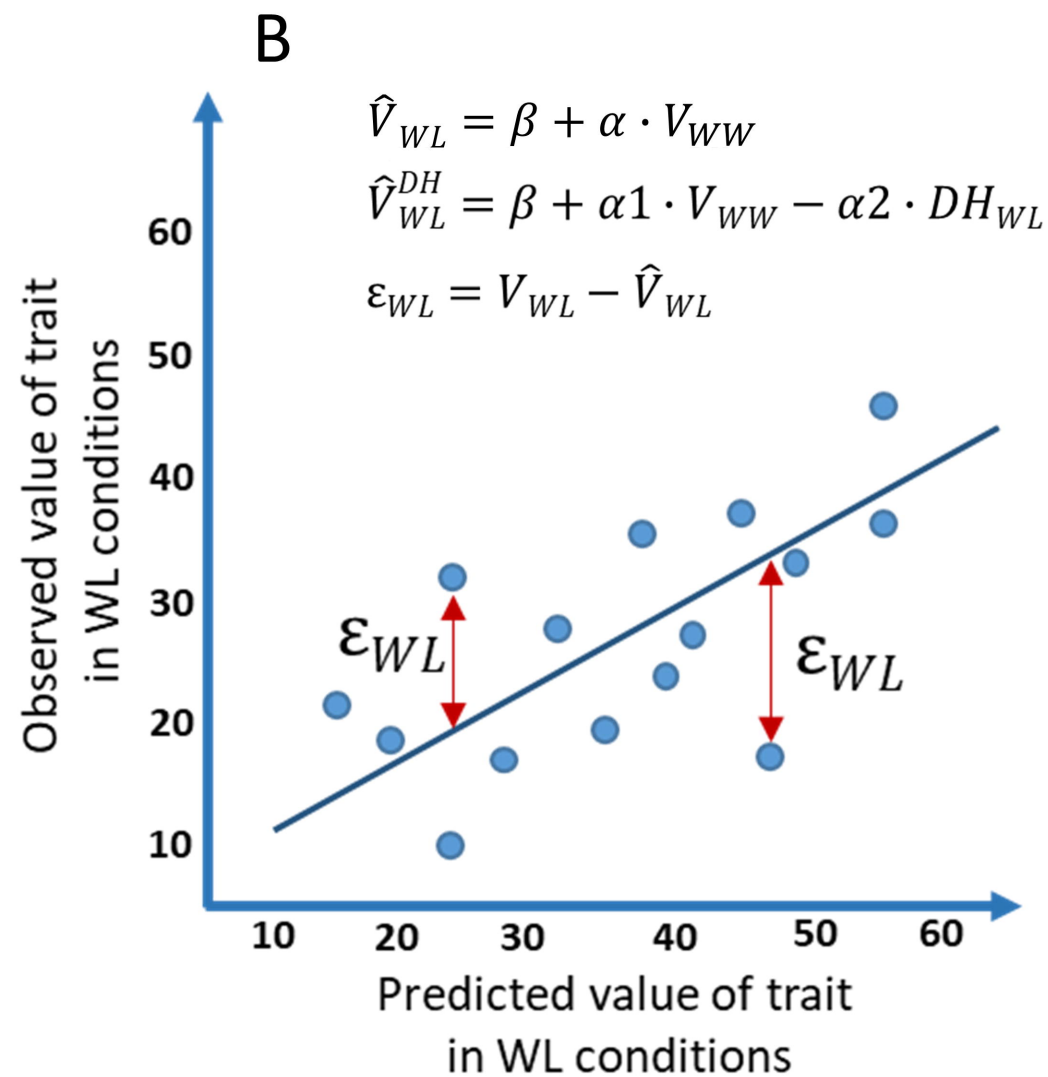
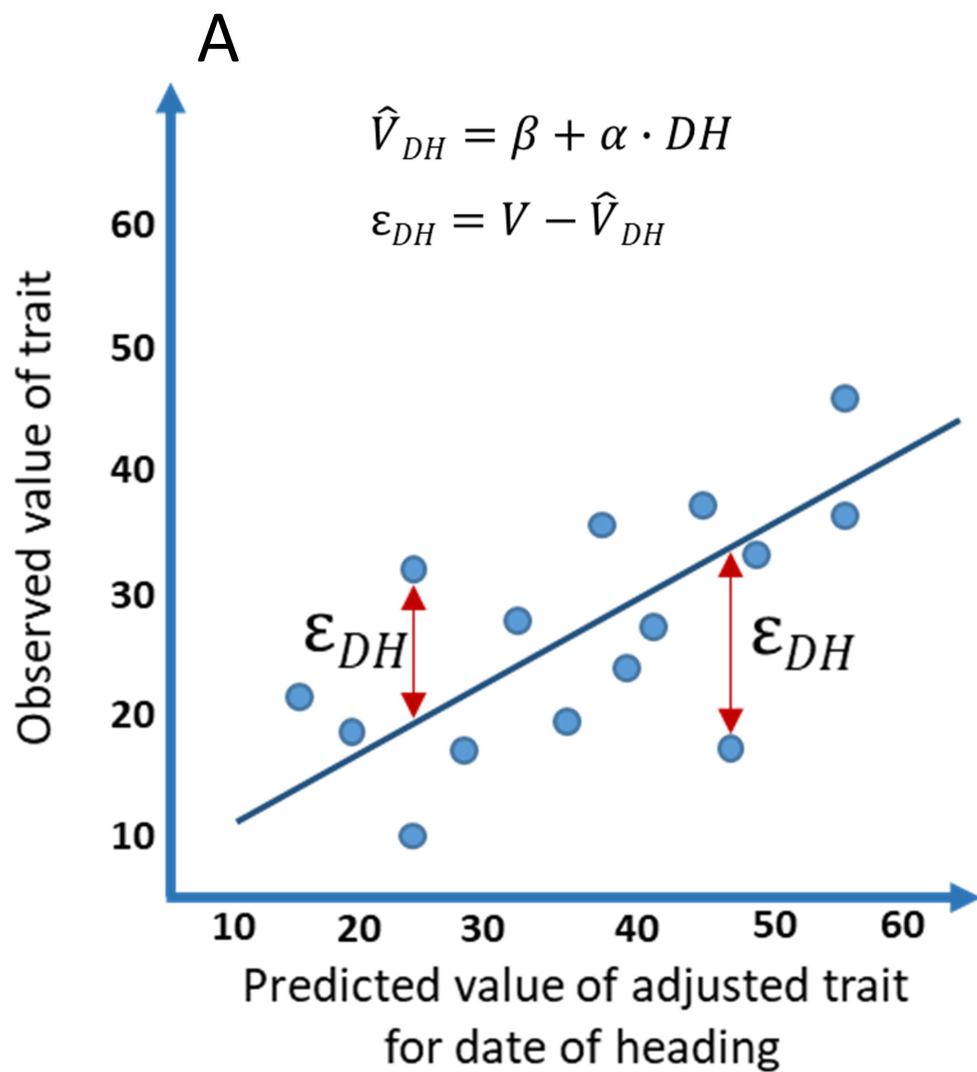
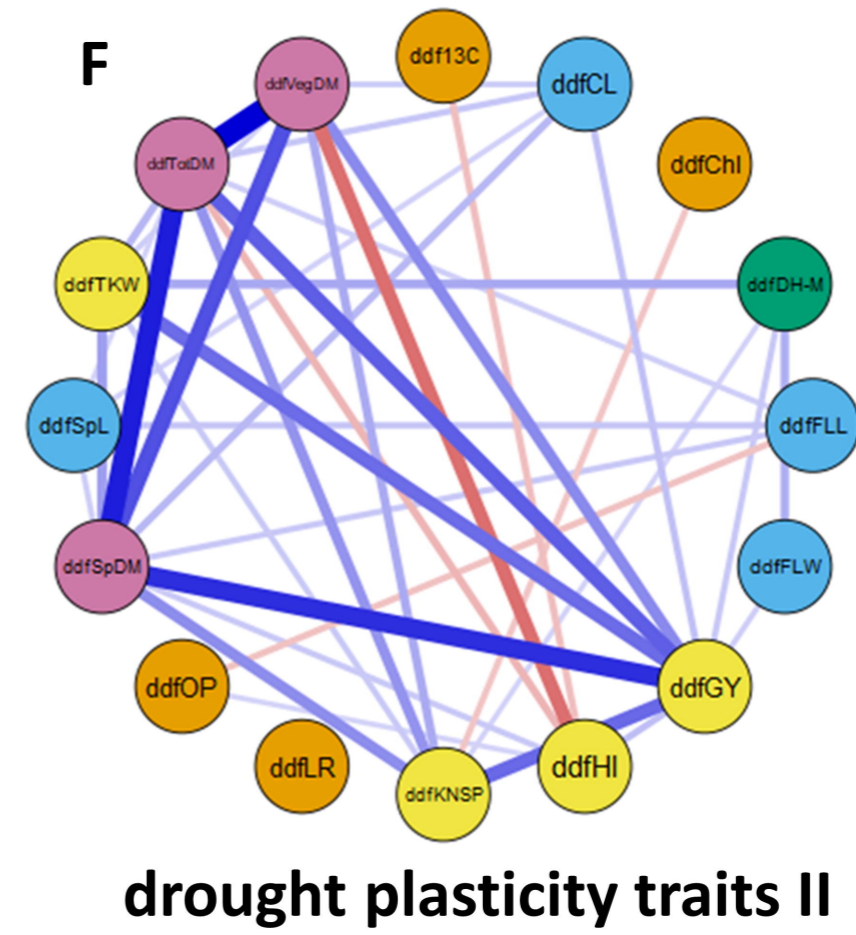
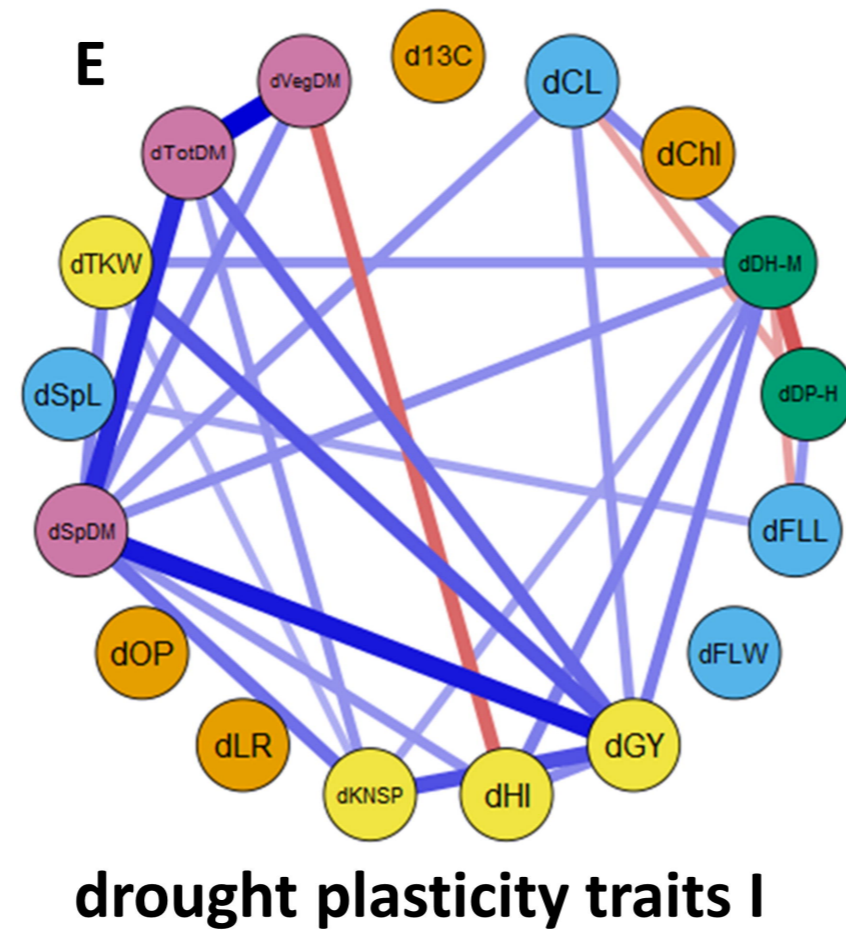
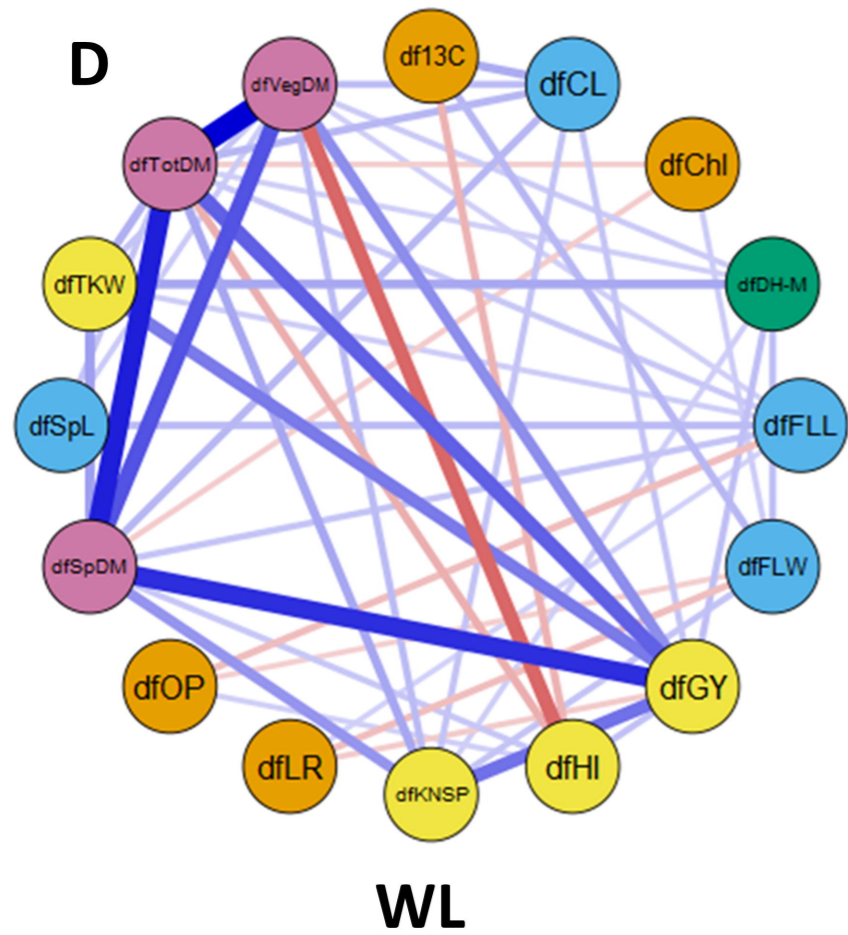
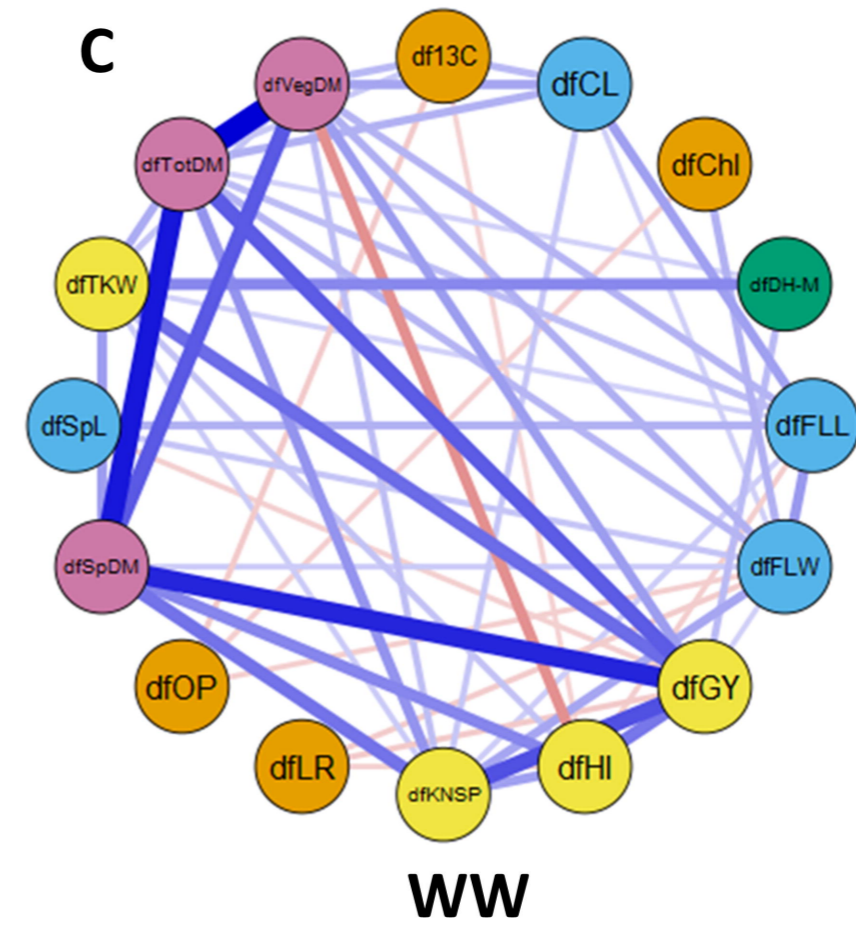
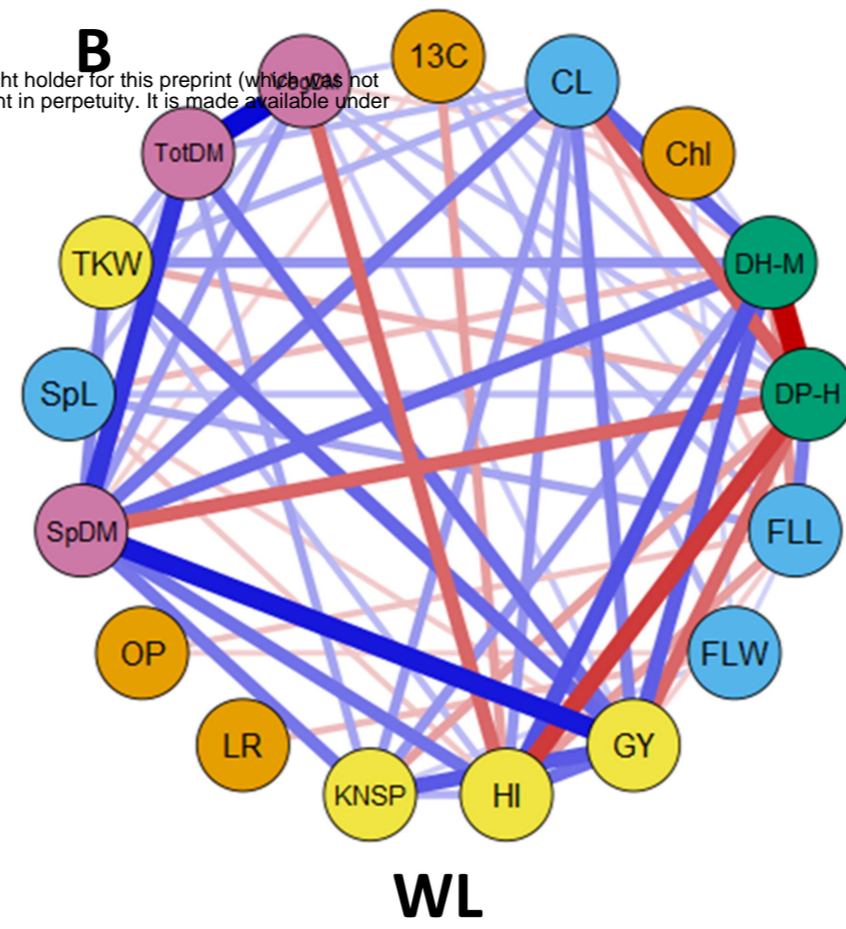
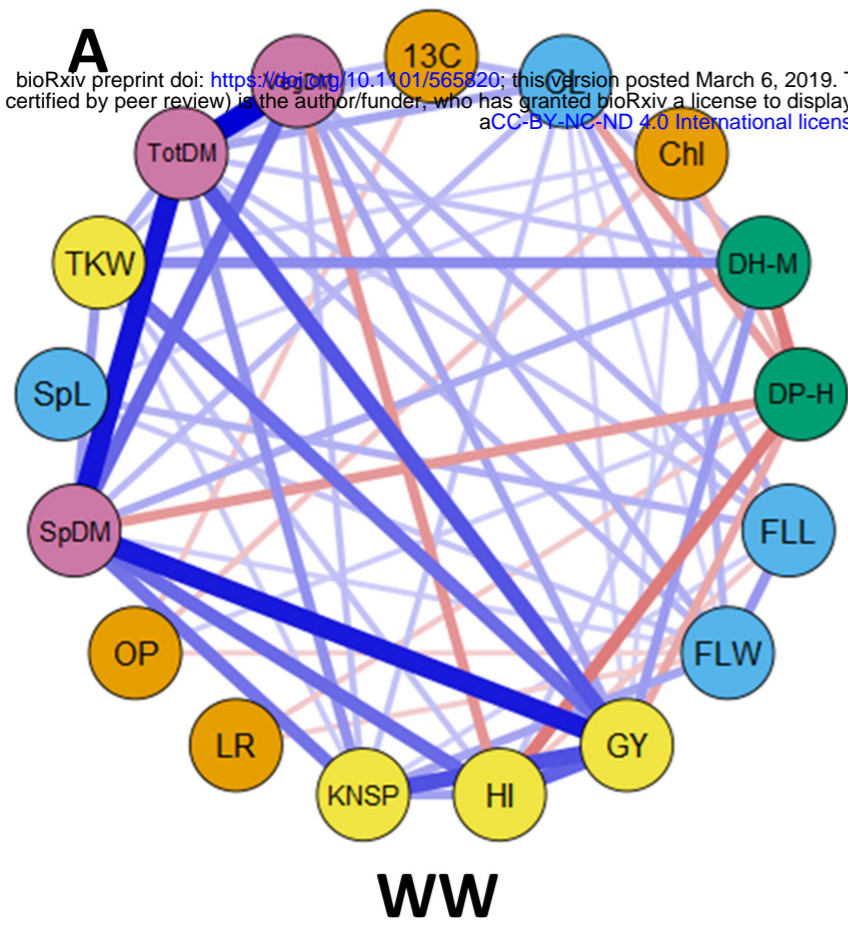


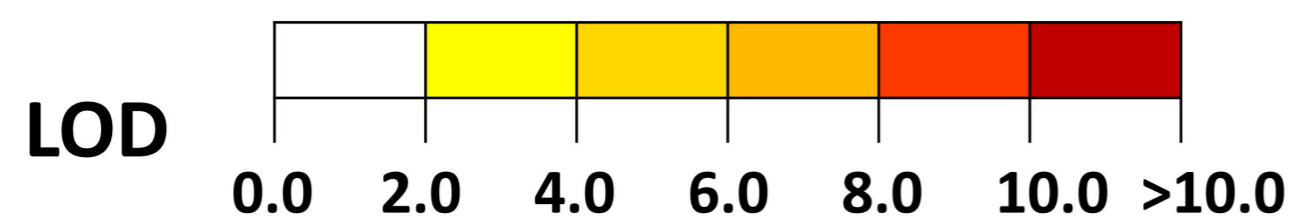
Fig. 4



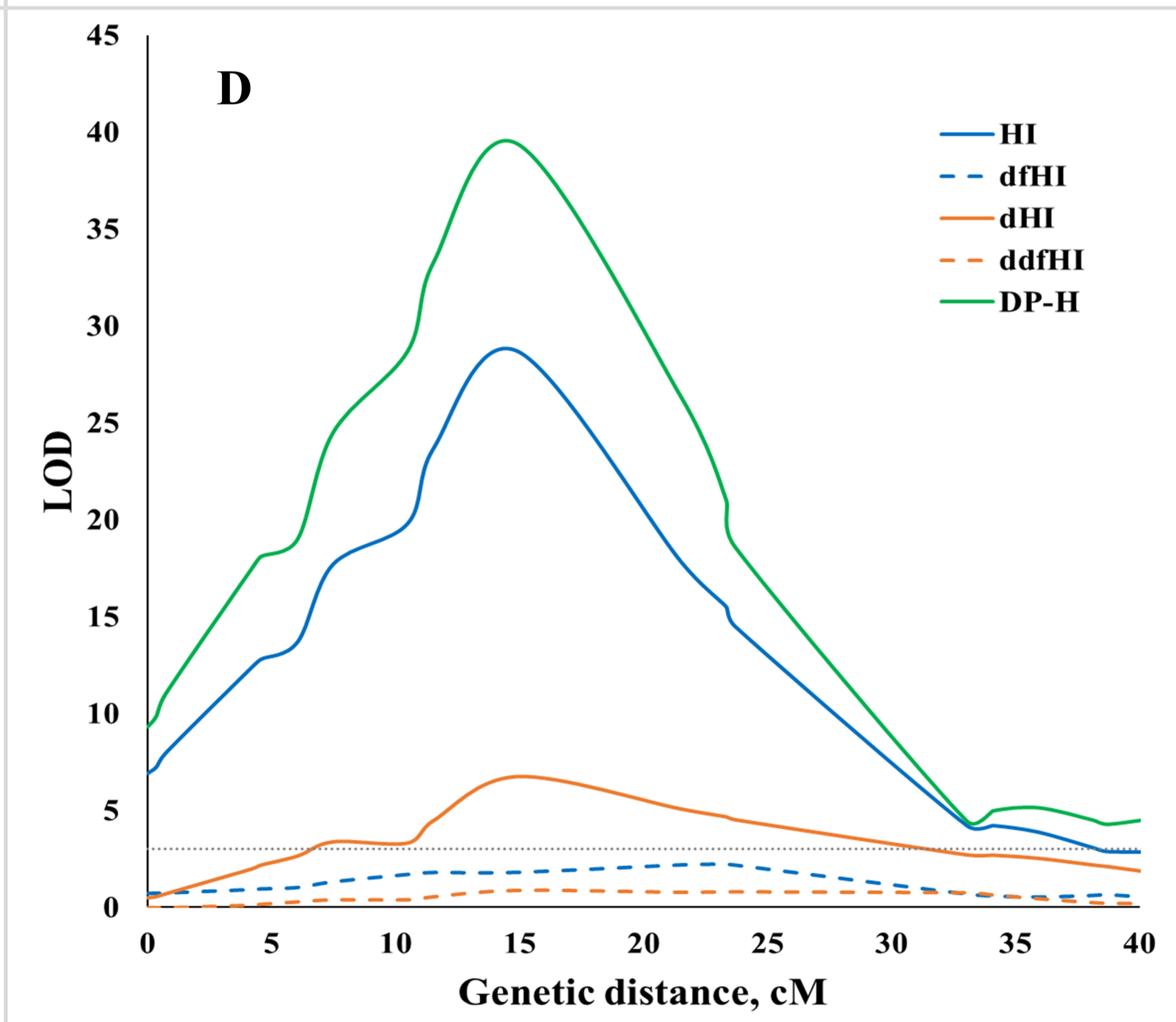
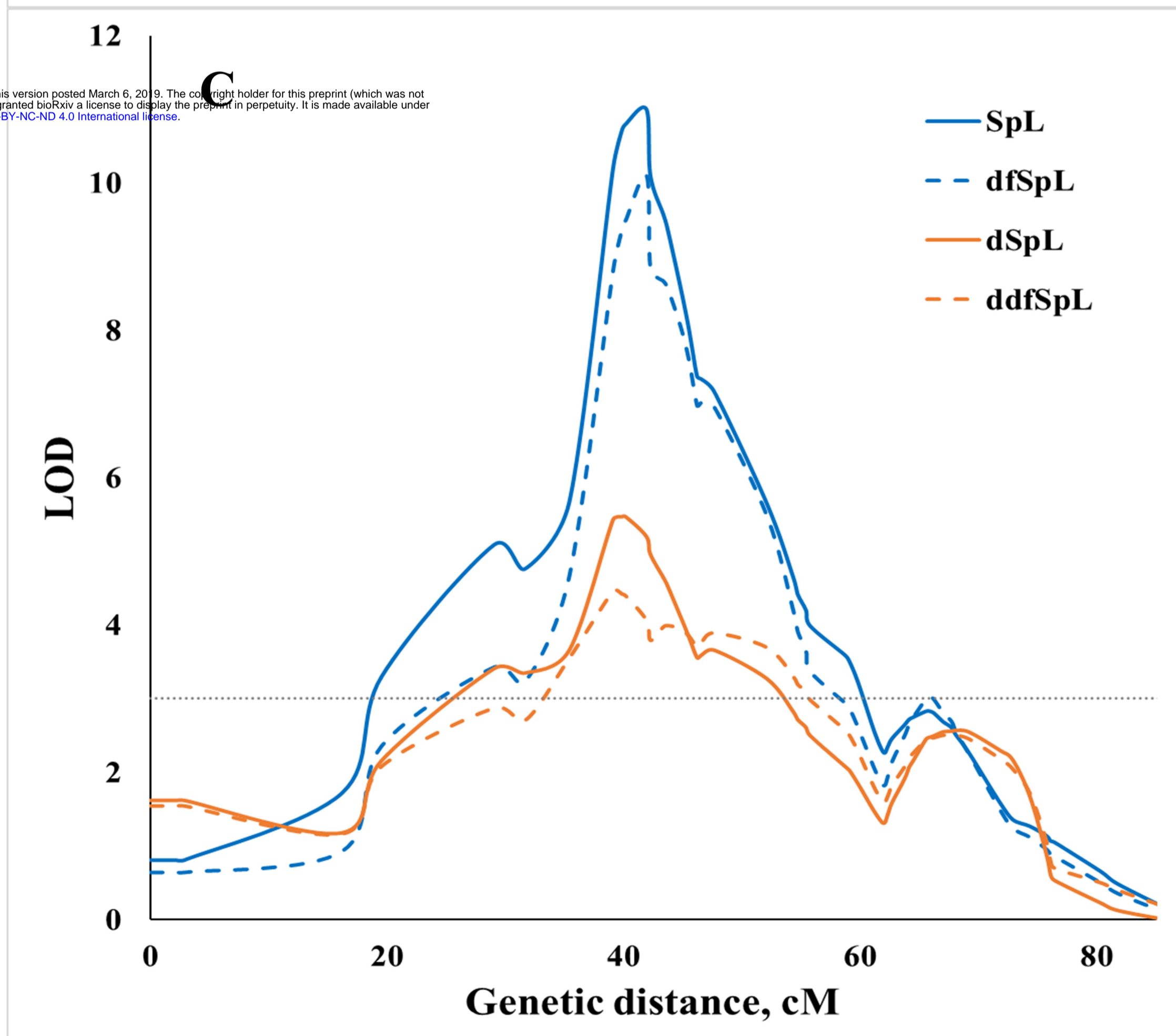
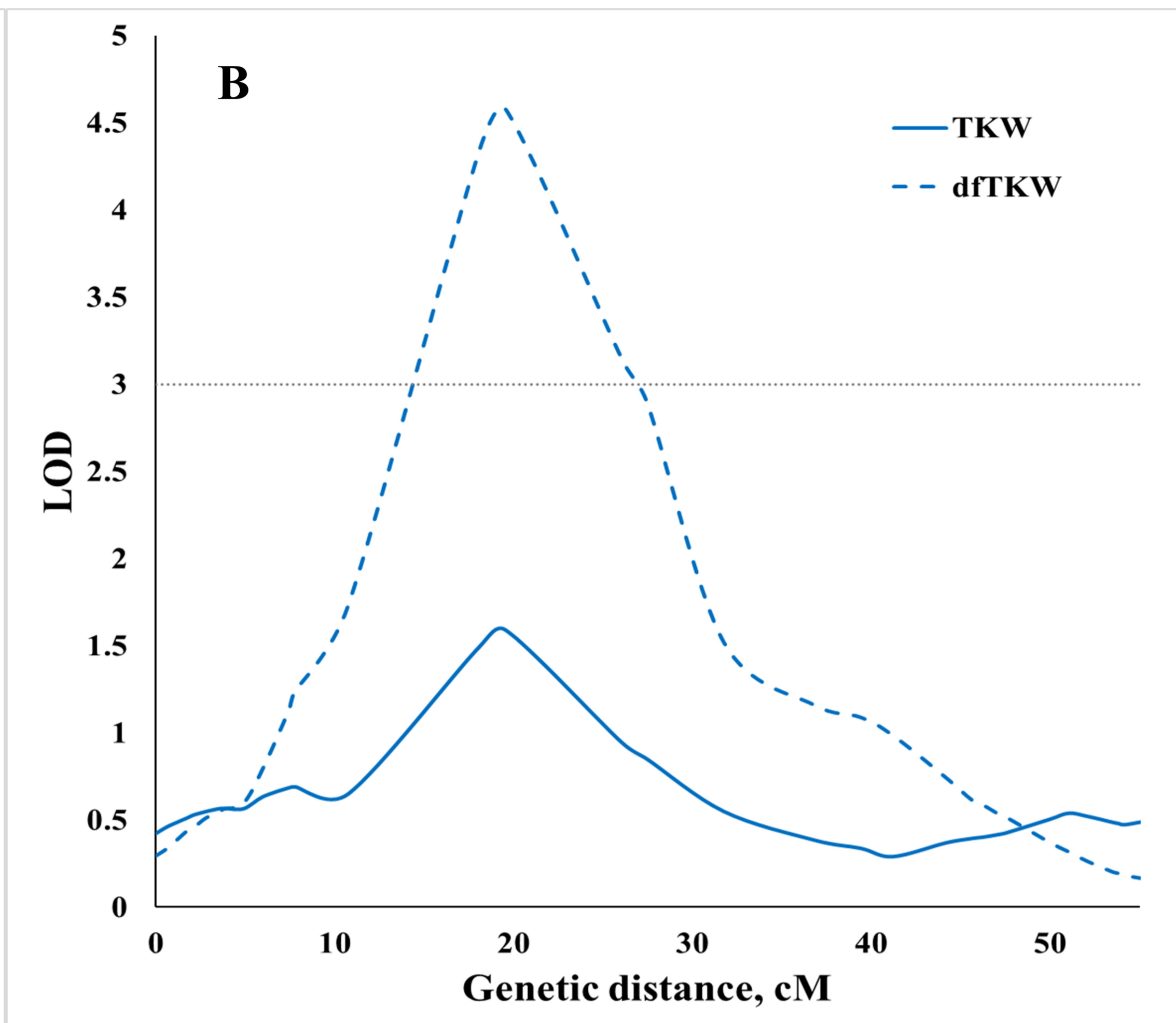
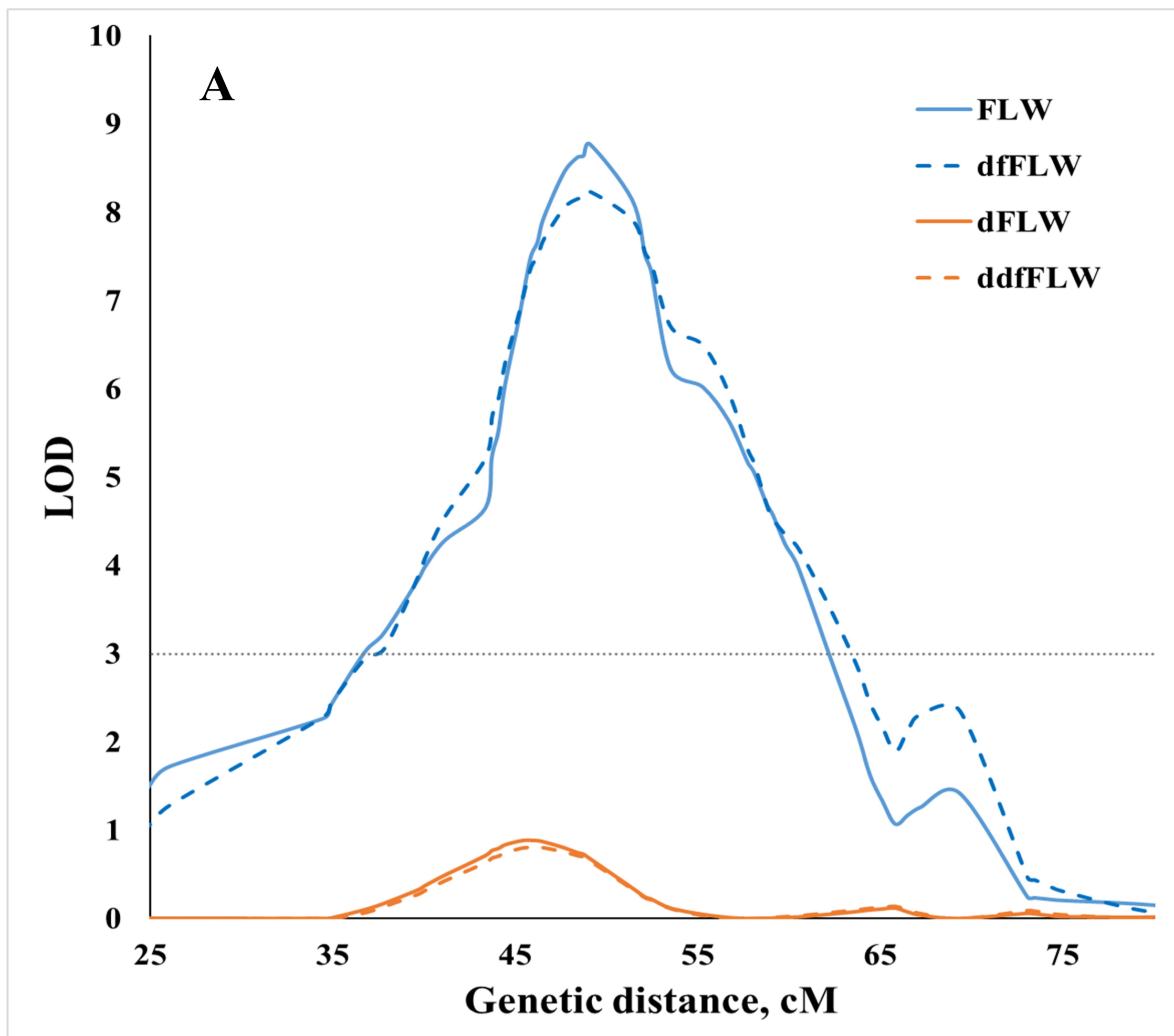


Traits

Chr.	QTLs	Plasticity to phenology			Traits																
		Plasticity to drought	Drought strategy		GY	TKW	KNSP	HI	SpDM	VeGDM	TotDM	CL	SpL	FLL	FLW	δ13C	OP	Chl	LR	DP-H	DH-M
1A	1A.1	P	NP	N												L					
	1A.2	NP	NP	A								G			L						
	1A.3	P	P	T		G*	L*									L*					
	1A.4	P	P	N				G**													
1B	1B.1	A	NP	N									L								L
	1B.2	NP	NP	N		L															
	1B.3	NP	P	A															L**		
2A	2A.1	P	NP	N	L*		L		L*	L	L										
	2A.2	P	NP	Ch										L			L				
	2A.3	NP	NP	T												L					
	2A.4	NP	NP	N									G								
	2A.5	NP	NP	A									L							G	
2B	2B.1	P	NP	N		G															
	2B.2	NP	NP	N	G			G													
	2B.3	P	NP	Ch, T												L	L*				
	2B.4	NP	P	N		G	L											L			
	2B.5	NP	NP	N														L			
	2B.6	A	P	E	L		L	L	L		L	L			L					G	L
	2B.7	NP	P	N		L**									L						
3A	3A.1	NP	P	A										G	L						
	3A.2	A	NP	N		G															
	3A.3	A	NP	N																L	
	3A.4	P	NP	Ch								L						G			
	3A.5	NP	NP	A										L		G					
	3A.6	P	NP	N			L*														
3B	3B.1	P	P	N				L*													
	3B.2	NP	P	T	L							L**					L				
	3B.3	A	NP	N								L									
	3B.4	NP	NP	N											G						
4A	4A.1	P	P	N				G		L	L										
	4A.2	P	P	Ch														G**			
	4A.3	P	P	A		L						L	L			G					L
	4A.4	P	P	N		L*															
	4A.5	P	NP	N												GL					
	4A.6	P	NP	N	L			L					G								
	4A.7	NP	P	N											G						
4B	4B.1	P	P	Ch					L**									G			
	4B.2	P	NP	Ch														G*			
	4B.3	NP	P	N	L	L			L	L	L										
	4B.4	A	NP	N								L		G							G
	4B.5	NP	P	T											L						
	4B.6	P	NP	N								L*									
5A	5A.1	P	NP	N		G*															
	5A.2	NP	P	N				L**		G	G										
	5A.3	P	P	A	L		L	L	L			L**	G	G				L	G	G	L
	5A.4	P	NP	A											G						
	5A.5	A	P	N											L					L	
	5A.6	P	P	T				G				G						L**			
	5A.7	A	P	A			L										G**				
	5A.8	A	P	E										L						L	G
	5A.9	P	NP	N								L*									
5B	5B.1	NP	NP	N		G															
	5B.2	P	NP	N											L*						
	5B.3	A	NP	N					G											G	
	5B.4	A	NP	N				G													
	5B.5	NP	NP	T												L					
	5B.6	NP	NP	Ch														G			
	5B.7	A	NP	N													G*			L	G
	5B.8	A	NP	N								G	G				G				
6A	6A.1	A	P	E				L**						L							G
	6A.2	P	P	Ch																L	
	6A.3	NP	NP	T		G											G				
	6A.4	P	P	Ch										L	L					G*	
6B	6B.1	A	NP	N																	L
	6B.2	P	P	T									L	G*				L			
	6B.3	NP	NP	N		L															L
	6B.4	NP	NP	A				G							L	G					
	6B.5	P	NP	Ch																G*	
7A	7A.1	P	NP	N					L	L	L										
	7A.2	P	NP	N		L*															
	7A.3	NP	NP	N						G				L							
	7A.4	NP	P	A																L	
	7A.5	P	NP	N		G							L	G							
	7A.6	P	NP	N			L									G*			G		
	7A.7	P	P	N																L**	
7B	7B.1	A	P	E	G	G	G	G	G			G	L							L	G
	7B.2	NP	P	A																	
	7B.3	NP	P	N															L**		
	7B.4	P	P	Ch			G**		G**						L				L*		



bioRxiv preprint doi: <https://doi.org/10.1101/568520>; this version posted March 6, 2019. The copyright holder for this preprint (which was not certified by peer review) is the author/funder, who has granted bioRxiv a license to display the preprint in perpetuity. It is made available under aCC-BY-NC-ND 4.0 International license.



bioRxiv preprint doi: <https://doi.org/10.1101/565520>; this version posted March 6, 2019. The copyright holder for this preprint (which was not certified by peer review) is the author/funder, who has granted bioRxiv a license to display the preprint in perpetuity. It is made available under aCC-BY-NC-ND 4.0 International license.